

Figure 5.1: A plot of cycle number vs the magnitude of the signal intensity (indicated by delta Rn) for different initial concentrations of DNA with a sequence specific to the GPCR43 transcript.

Initial results for Q-PCR experiment using serial dilutions of a known concentration of GPCR43 full length template (10^7 - 10^1 copies). Shown is the cycling threshold (Ct) which is the point at which the reaction is in the linear phase and the fluorescence can be detected above the background fluorescence.

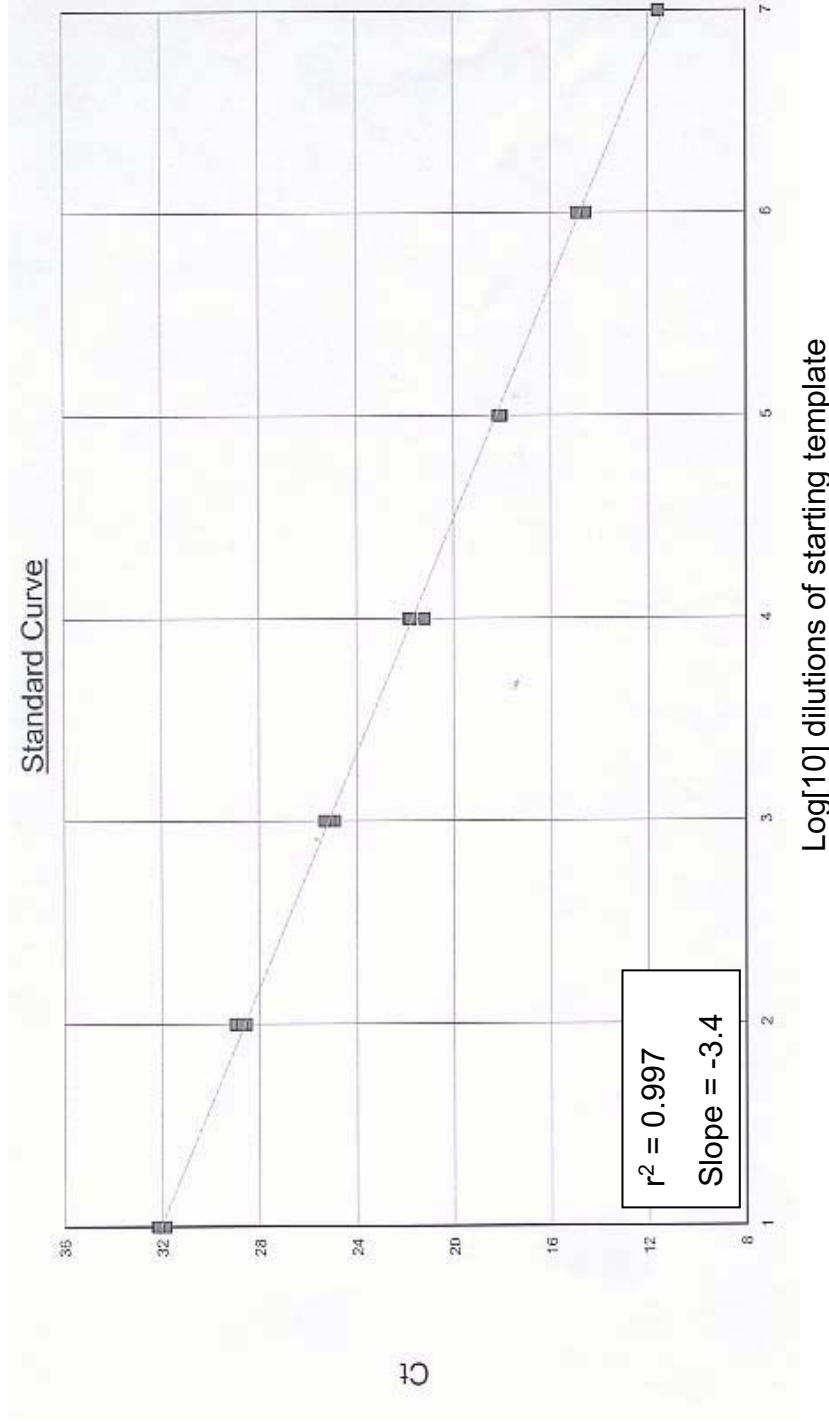


Figure 5.2: A plot of Log dilutions of starting template vs Ct values (derived from Figure 5.1).

The standard curve for Q-PCR reactions generated using serial dilutions of a known concentration of GPCR43 full length template. The co-efficient of determination (r^2) value and the slope of the line have been indicated.

Figure 5.3: Gel electrophoresis analysis of standard curve amplicons generated using Q-PCR.

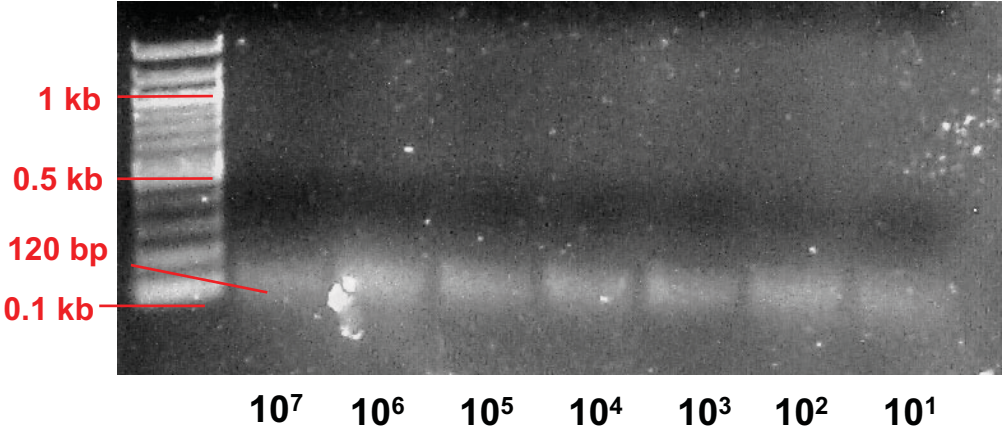
Shown in panel (a) are Q-PCR amplicons generated from the GPCR43 standard curve (from Figure 5.1) illustrating bands of approximately 120 base pairs which decrease in intensity with a decreased concentration of starting template. No other contaminating bands are present indicating no inhibition of the Q-PCR reaction occurred due to non-specific amplification.

Shown in panel (b) is the quantification of gel image in using Scion Image.

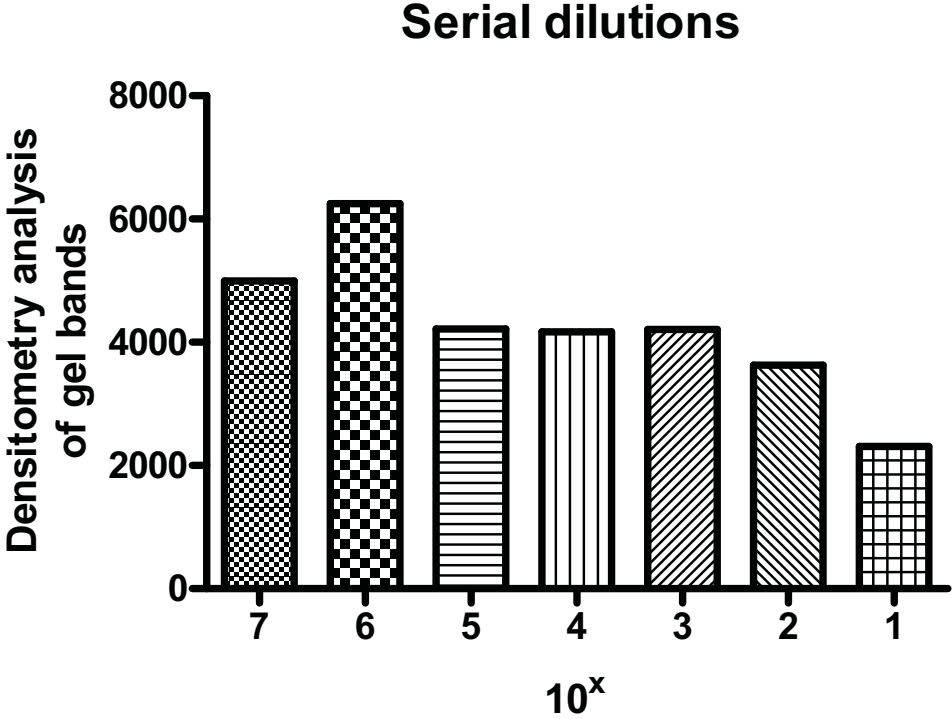
The molecular weight markers are shown with the precise details described in the text.

Figure 5.3

a



b





1 atgctgccgg actggaagag ctccttgatc ctcatggctt acatcatcat cttcctcact
 61 ggccctccctg ccaacctcct ggccctgccg gcctttgtgg ggcggatccg ccagccccag
 121 cctgcacctg tgcacatcct cctgctgagc ctgacgctgg ccgacctcct cctgctgctg
 181 ctgctgccct tcaagatcat cgaggctgag tcgaacttcc gctggtacct gcccaaggtc
 241 gtctgcgccc tcacgagttt tgctttctac agcagcatct actgcagcac gtggctcctg
 301 gcgggcatca gcatcgagcg ctacctggga gtggctttcc ccgtgcagta caagctctcc
 361 cgccggcctc tgtatggagt gattgcagct ctgggtggcct gggttatgtc ctttggtcac
 421 tgcaccatcg tgatcatcgt tcaatacttg aacacgactg agcaggtcag aagtggcaat
 481 gaaattacct gctacgagaa cttcaccgat aaccagttgg acgtgggtgct gcccgtagcg
 541 ctggagctgt gcctgggtgct cttcttcate cccatggcag tcaccatcct ctgctactgg
 601 cgttttgtgt ggatcatgct ctcccagccc cttgtggggg cccagaggcg gcgcccagcc

 661 gtggggctgg ctgtggtgac gctgctcaat ttcttgggtg gttcgggacc ttacaacgtg
 721 tcccacctgg tggggatca ccagagaaaa agccccctgt ggcgggtcaat agccgtggtg
 781 ttcagttcac tcaacgccag tctggacccc ctgctcttct atttctcttc ttcagtgggtg
 841 cgcagggcat ttgggagagg gctgcagggtg ctgcggaatc agggctcctc cctgttggga
 901 cgcagaggca aagacacagc agaggggaca aatgaggaca ggggtgtggg tcaaggagaa


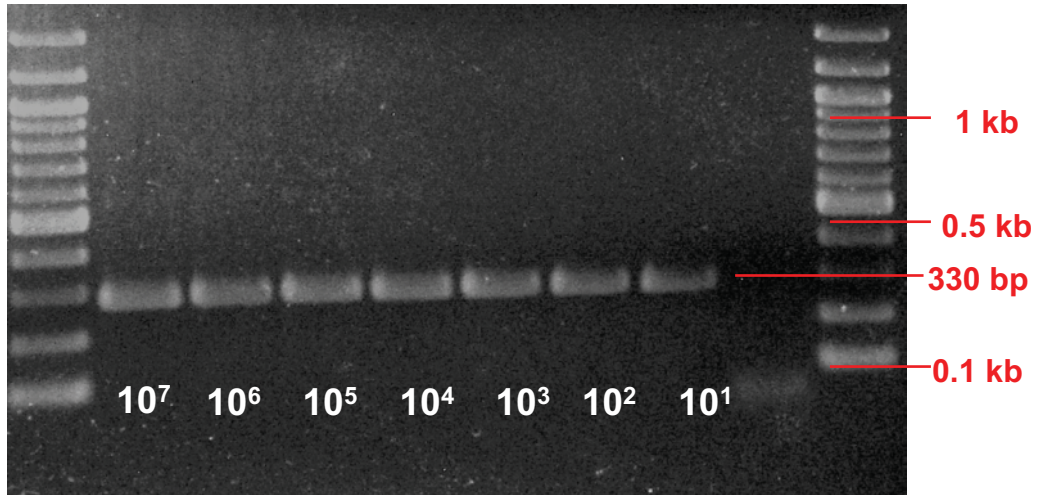
 961 gggatgccaa gttcggactt cactacagag tag


Figure 5.4: A representation of the GPCR43 mRNA transcript.

Arrows in blue indicate the position of the primers used to generate the full length GPCR43 amplicon to construct the standard curve. Arrows in green indicate the position of the nested primers used in the RT-PCR, with amplicon products electrophoresed in Figure 5.5.

Figure 5.5

a



b

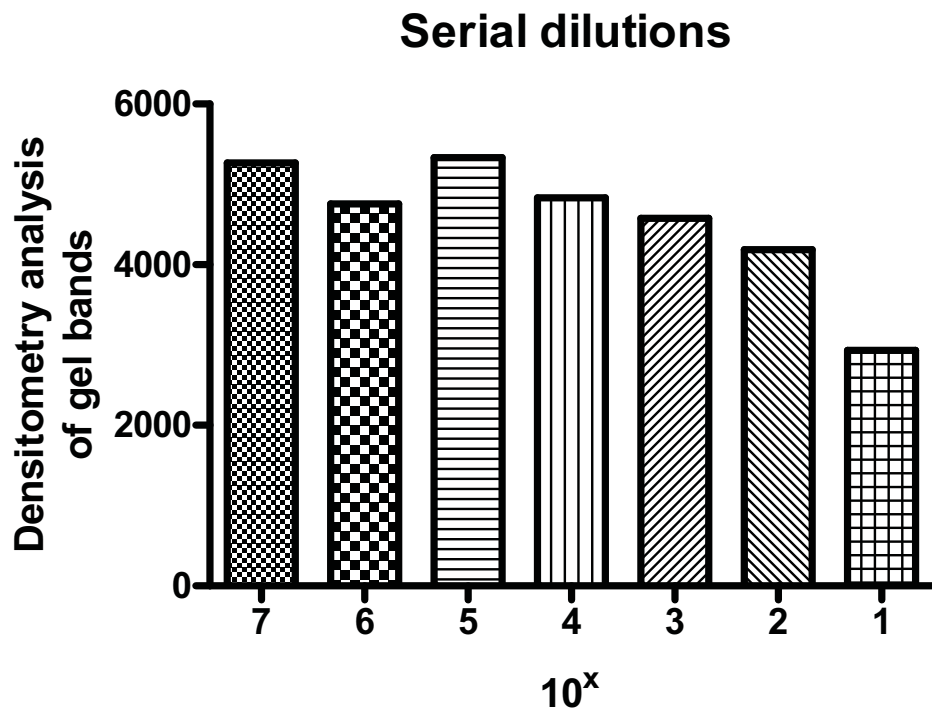
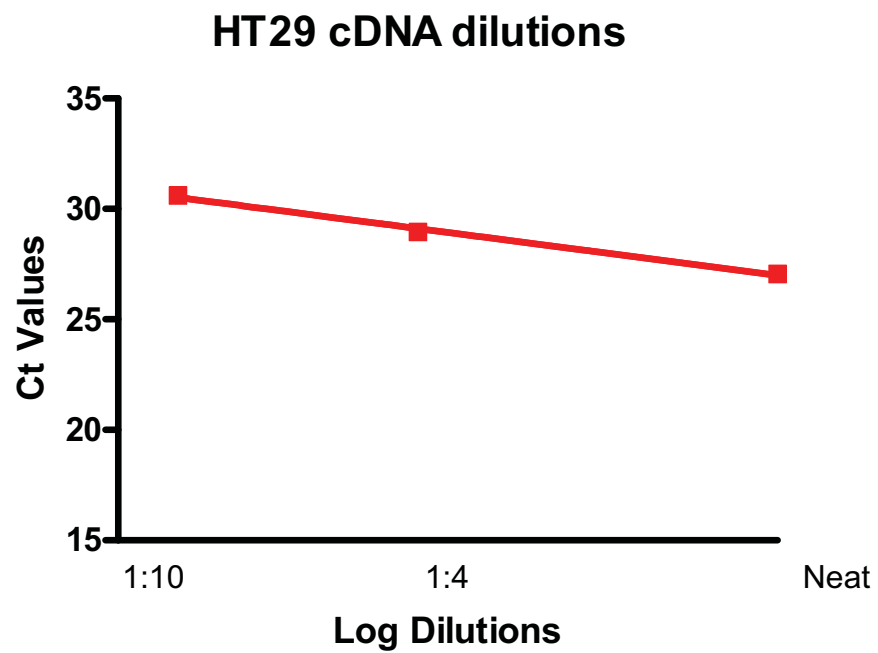


Figure 5.5: Gel electrophoresis analysis of standard curve amplicons generated using RT-PCR with nested primers.

Shown in panel (a) are the PCR amplicons generated from the GPCR43 standard curve of different concentrations of starting template using nested primers.

Panel (b) shows the quantification of gel image using Scion Image.

The dilutions are shown in both panels and the molecular weight markers are shown in (a). The precise details are described in the text.



Slope= -3.4 ± 0.3

Figure 5.6: A plot of Ct values and the log dilution of cDNA extracts from HT29 cells used to calculate reaction efficiency.

The log dilutions of the starting template amount and the Ct values are shown. The slope was determined using GraphPad Prism 5 for Windows software and has been presented.

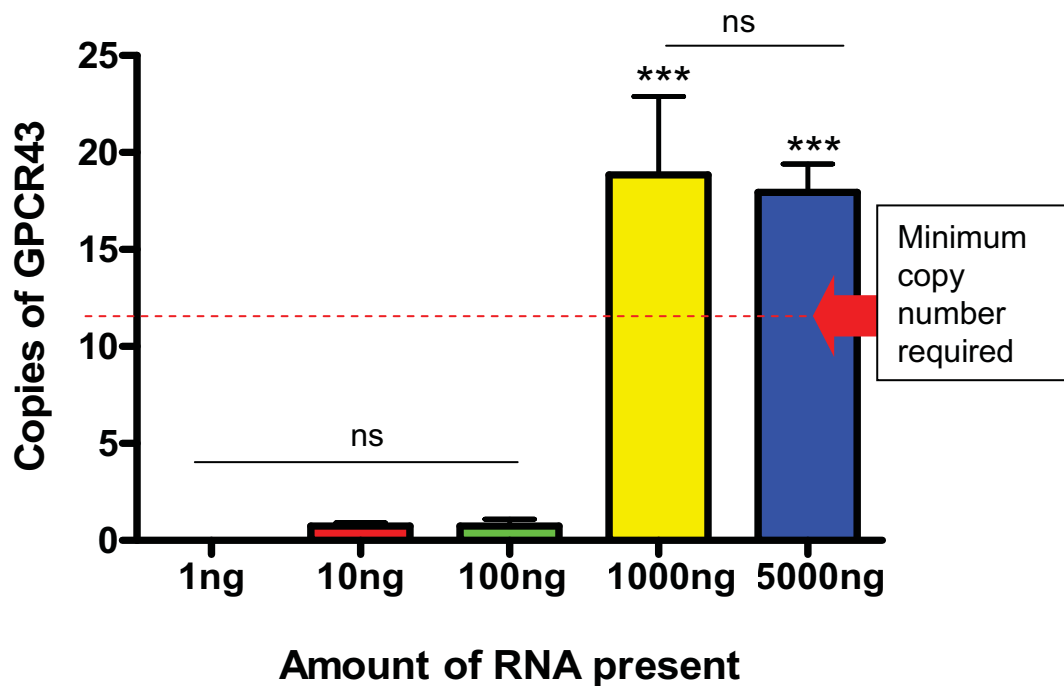


Figure 5.7: A plot of starting RNA concentration vs copies of GPCR43.

Increasing quantities of RNA were reverse transcribed to cDNA and run in a Q-PCR reaction. “Initial values” which are the copies of GPCR43 prior to correction for starting concentration are displayed. The dashed red line indicates the minimum value of the standard curve (10 copies). Shown is the mean ± SEM.

(***) $p < 0.001$ denotes significantly different from 1ng.

ns indicates not significantly different.

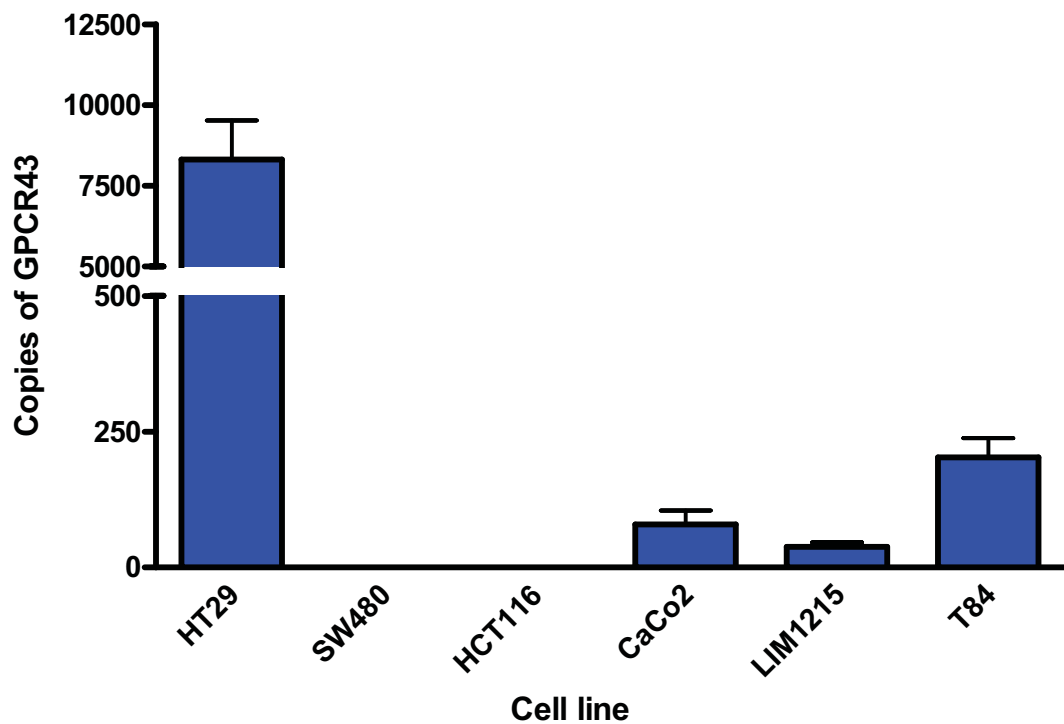


Figure 5.8: Copies of GPCR43 in 6 different CRC cell lines using a 1:10 dilution of cDNA template.

Shown is the expression of GPCR43 on 6 different CRC cell lines using Q-PCR and absolute quantitation. Shown is the mean \pm SEM.

Results show that GPCR43 is differentially expressed in 4 of 6 CRC cell lines, with highest expression in HT29 cells, then T84, CaCo2 and LIM1215 in decreasing levels of expression.

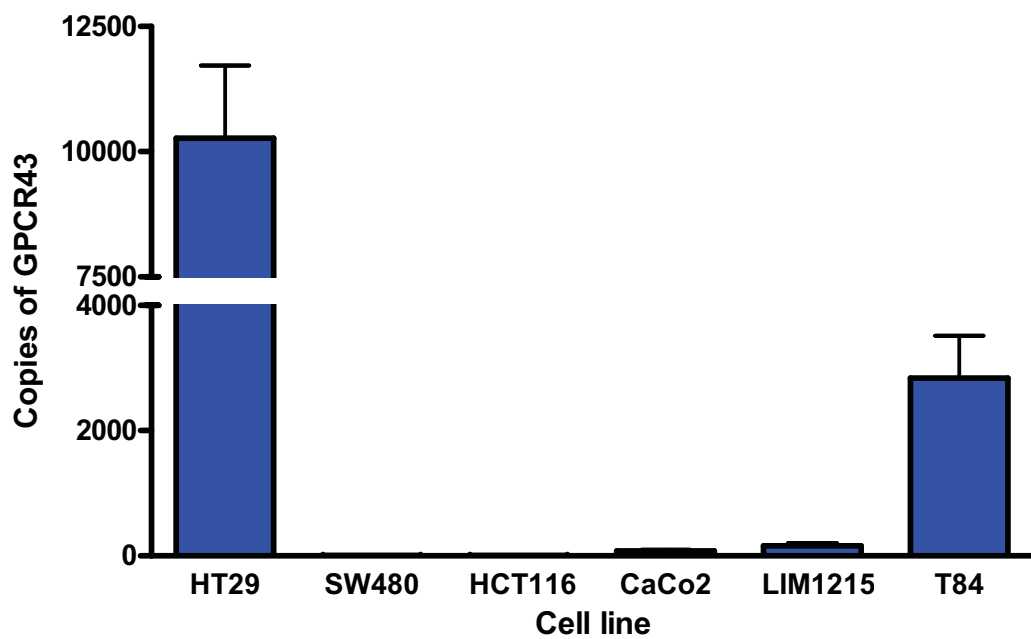


Figure 5.9: Copies of GPCR43 in 6 different CRC cell lines using an undiluted concentration of cDNA template.

Expression of GPCR43 on 6 different CRC cell lines using Q-PCR and absolute quantitation. Shown is the mean \pm SEM.

Results show that GPCR43 is differentially expressed in 4 of 6 CRC cell lines, with highest expression in HT29 cells, then T84, CaCo2 and LIM1215 in decreasing levels of expression.

Figure 5.10

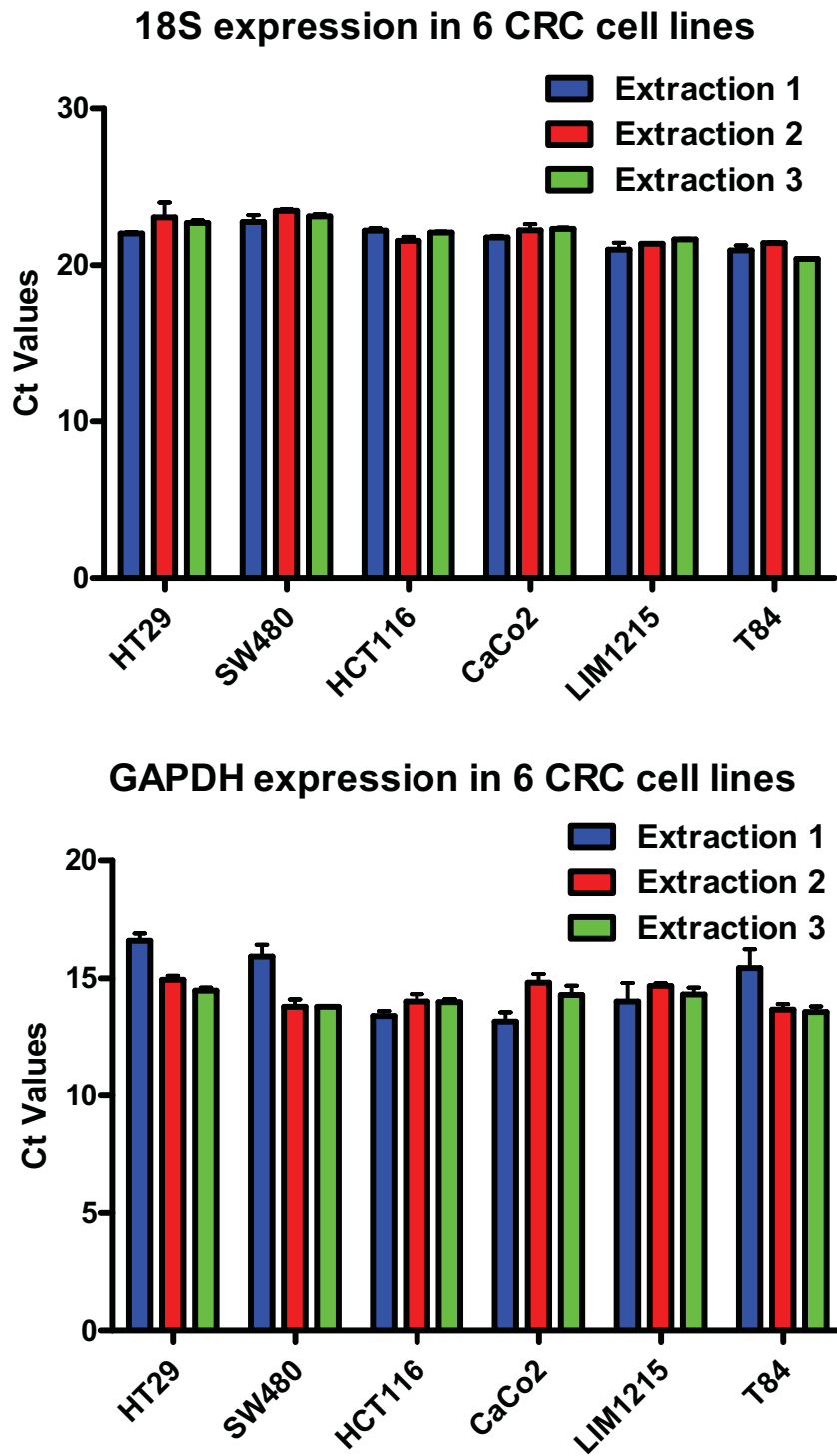


Figure 5.10: Expression of 18S and GAPDH housekeeping genes using cDNA extracted from 6 CRC cell lines.

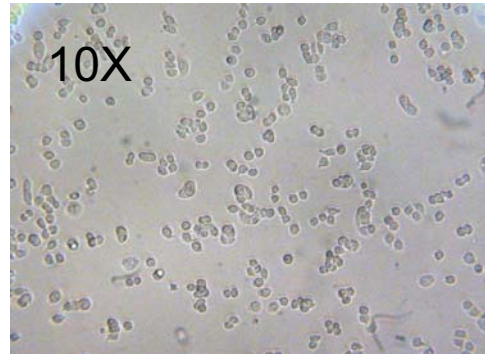
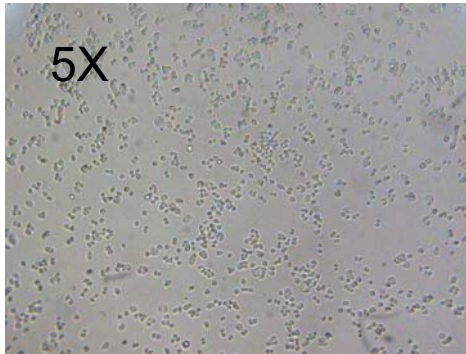
The upper panel summarises the expression of the 18S housekeeping gene from the 6 different CRC cell lines in 3 different Q-PCR experimental runs. Shown is the mean \pm SEM.

The lower panel summarises the expression of GAPDH from the 6 different CRC cell lines in 3 different Q-PCR experimental runs.

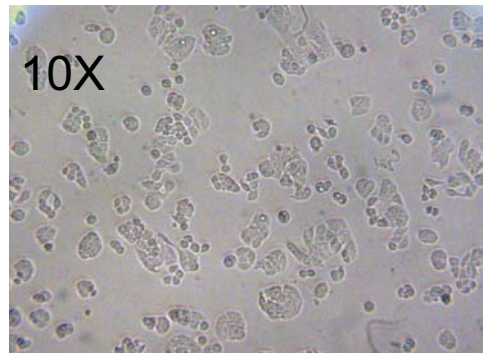
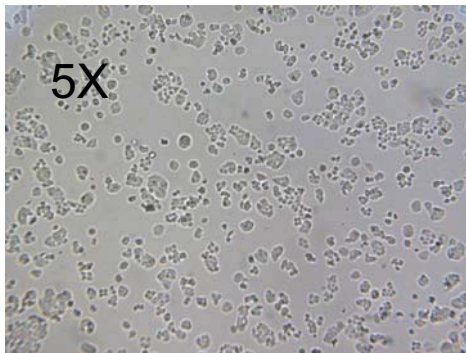
Results show that both 18S and GAPDH are constitutively expressed on each of the CRC cell lines.

Figure 6.1: Representative photomicrographs of HT29 cells at 24, 48 and 72 hours post seeding illustrating the extent of cell confluence at the time points tested at 2 magnifications.

24 hours post seeding: 20-30% confluence



48 hours post seeding: 40-50% confluence



72 hours post seeding: 80-90% confluence

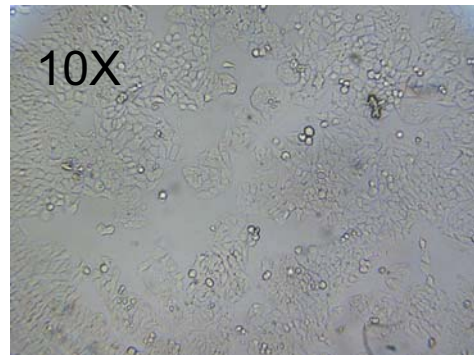
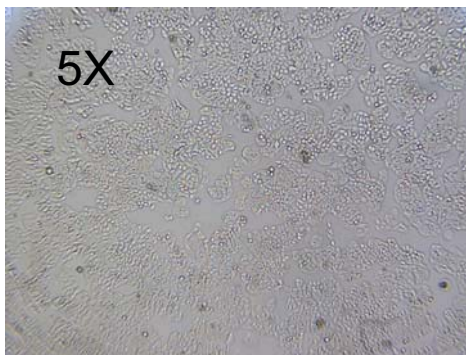
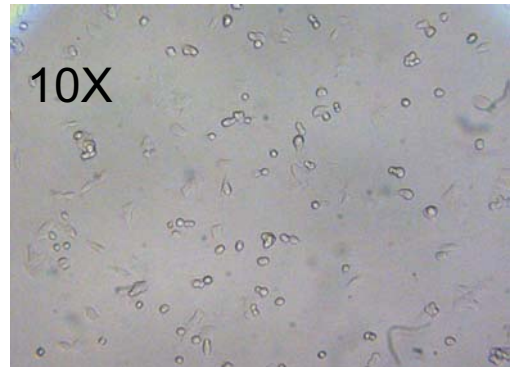
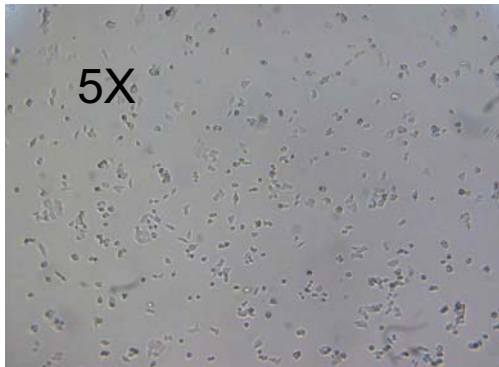
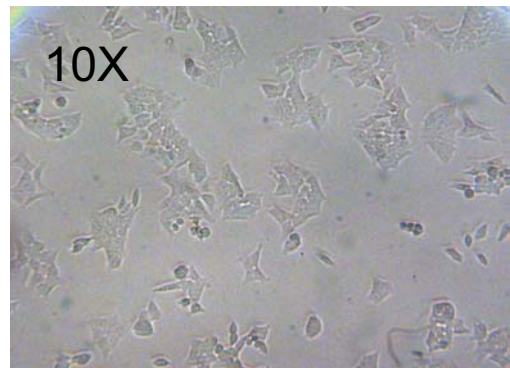
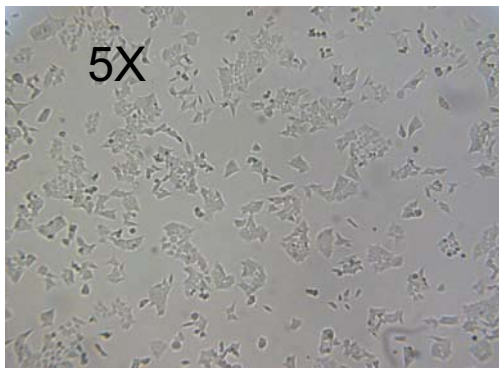


Figure 6.2: Representative photomicrographs of HCT116 cells at 24, 48 and 72 hours post seeding illustrating the extent of cell confluence at the time points tested at 2 magnifications.

24 hours post seeding: 20-30% confluence



48 hours post seeding: 40-50% confluence



72 hours post seeding: 80-90% confluence

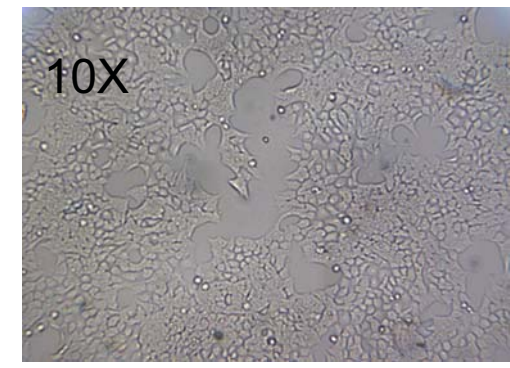
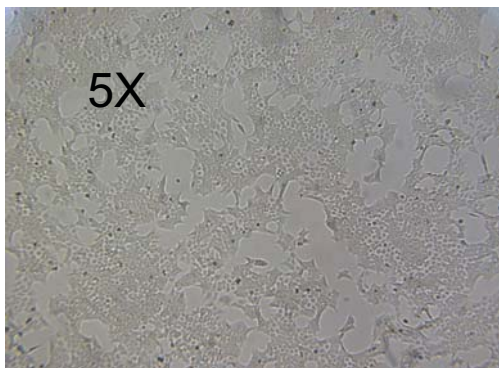


Figure 6.3: The influence of cell confluency on GPCR43 gene expression in HT29 and HCT116 cells.

Shown in panel (a) is the expression of GPCR43 in HT29 cells grown to 20-30%, 40-50% or 80-90% confluence as described in the text. Panel (b) shows the same parameters in HCT116 cells.

The mean values \pm SEM are presented.

No observable differences were detected between any confluency using One-Way ANOVAs with Tukey's post hoc testing (significance set at $p < 0.05$).

Figure 6.3

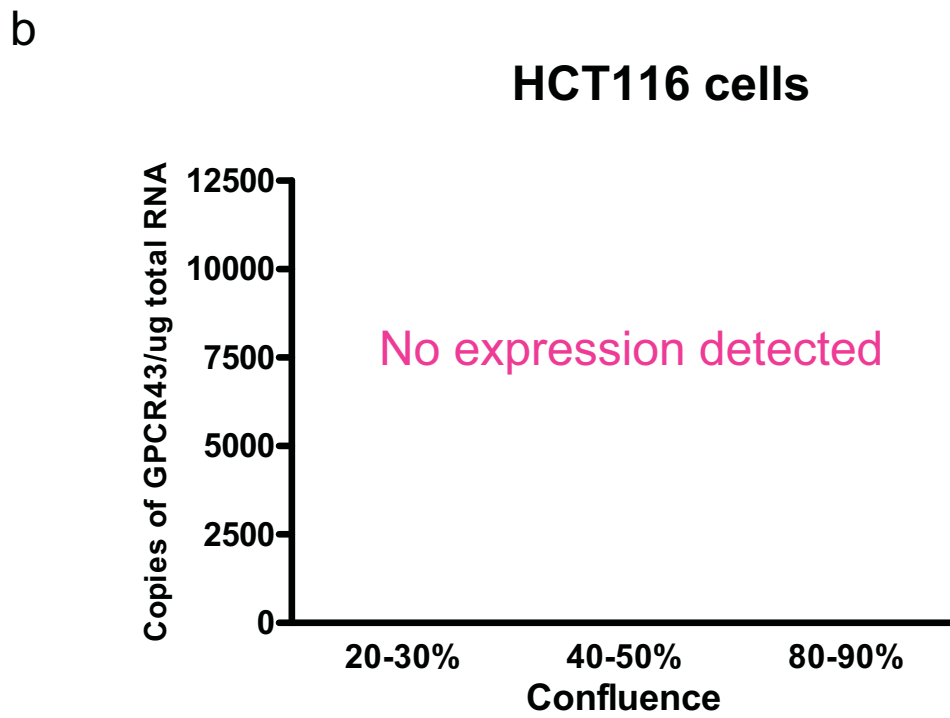
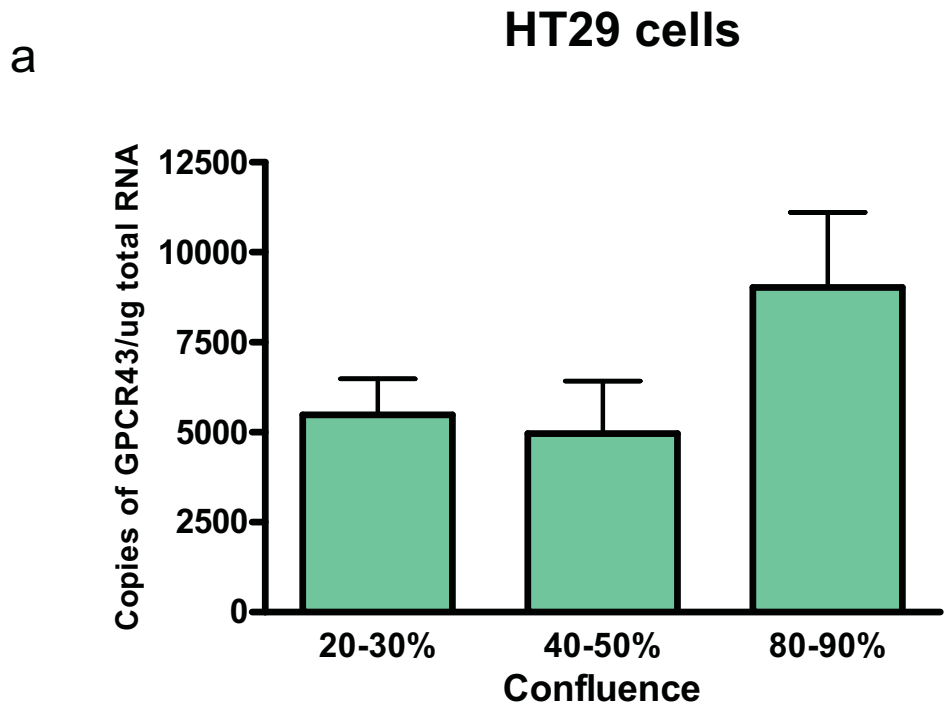


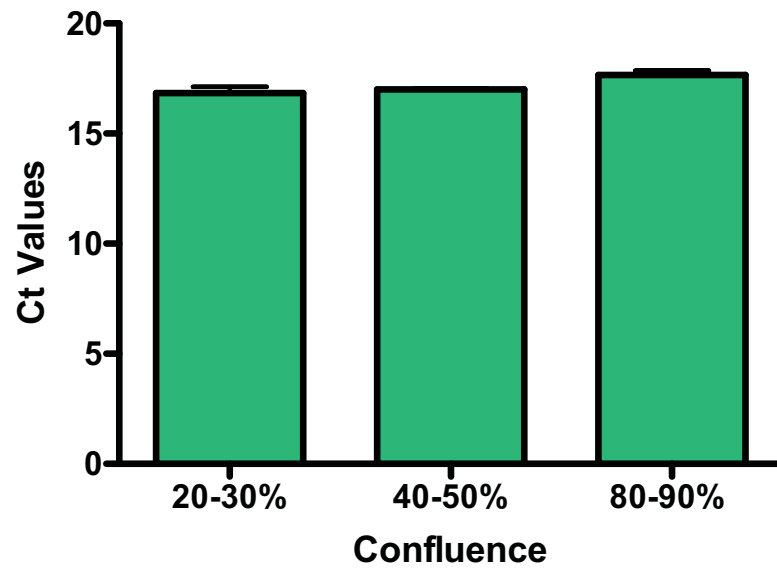
Figure 6.4: The influence of cell confluence on 18S expression in HT29 and HCT116 cells.

Shown in panel (a) is the expression of 18S on HT29 cells and in panel (b) HCT116 cells grown to 20-30%, 40-50% or 80-90% confluence. Shown is the mean \pm SEM.

Consistent expression of 18S is observed at each cell confluence in both HT29 cells and HCT116 cells.

Figure 6.4

a **18S Expression in HT29 cells with increasing cell confluence**



b **18S Expression in HCT116 cells with increasing cell confluence**

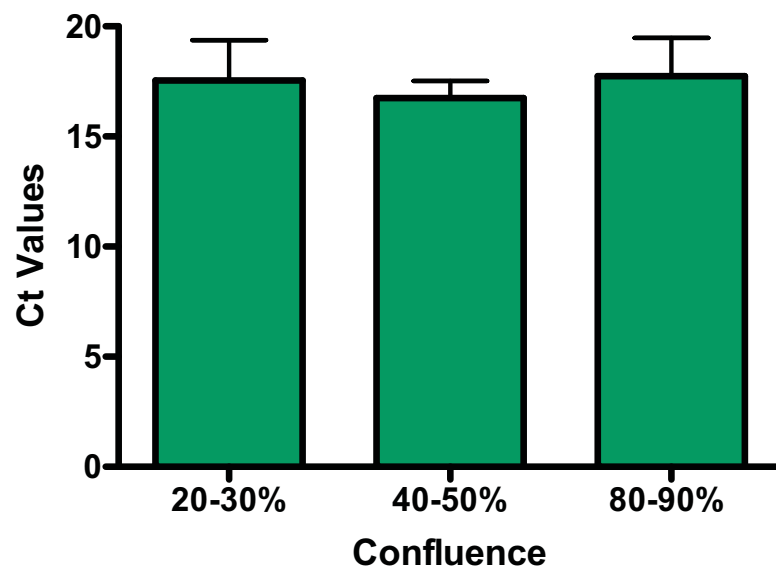


Figure 6.5: The influence of cell confluence on Alkaline Phosphatase Activity in HT29 cells.

The Alkaline Phosphatase activity of HT29 cells grown to 20-30%, 40-50% or 80-90% cell confluence. Shown are the mean values \pm SEM. A reaction free of HT29 lysate provided the control in the experimentation.

No significance differences were detected between any confluency using One-Way ANOVAs were performed with Tukey's post hoc testing (significance determined as values $p < 0.05$).

Figure 6.5

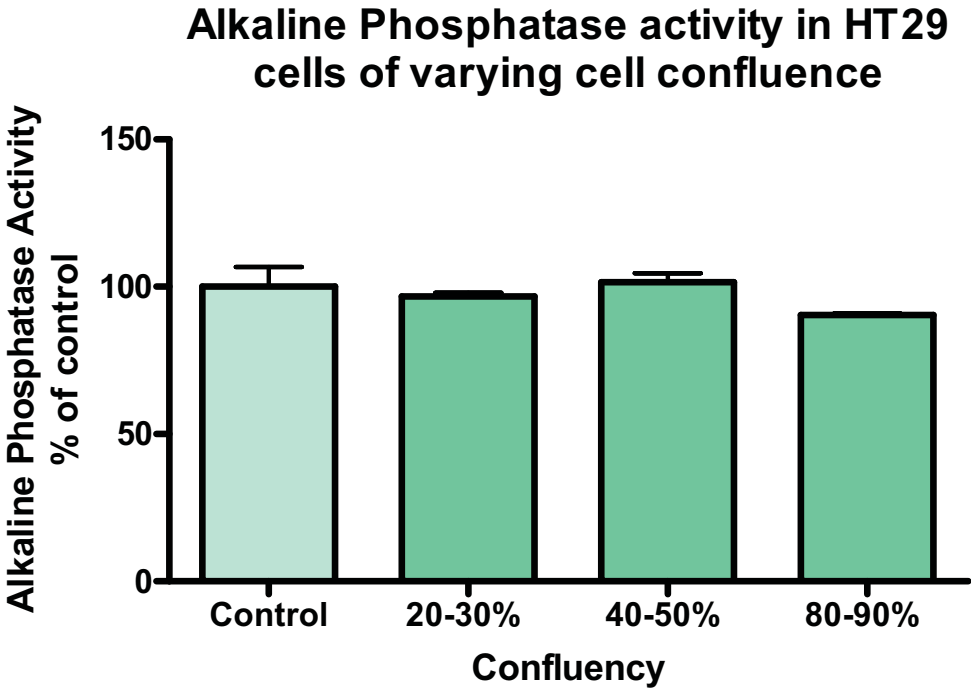


Figure 6.6: Alkaline Phosphatase activity in HT29 cells following exposure to 5mM BuA.

Shown are the mean values \pm SEM. Controls in the experimentation included HT29 lysate-free and HT29 cells grown in normal growth media free from BuA. HT29 cells exposed to 5mM BuA for 48 hours showed significantly greater levels of Alkaline Phosphatase activity compared to each control.

Significance was determined using One-Way ANOVAs were performed with Tukey's post hoc testing (significance set at $p < 0.05$).

(***) $p < 0.001$ denotes significance compared to 0mM BuA and control.

Figure 6.6

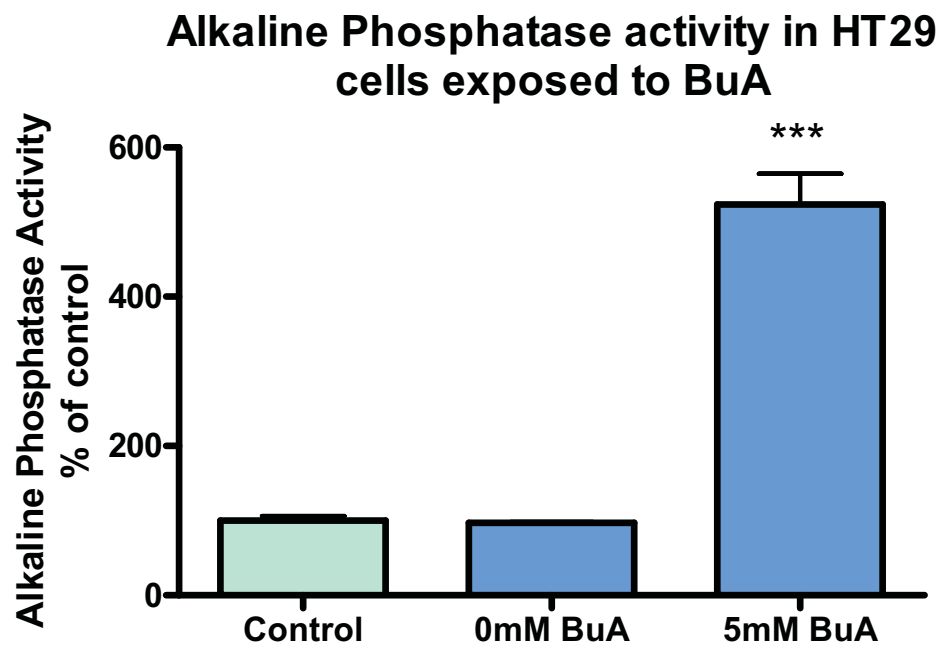


Figure 7.1: Representative photomicrographs of HT29 and HCT116 cells illustrating the changes in cell morphology induced by BuA exposure for 24 hours.

Shown are different magnitudes of untreated and BuA-treated cells.

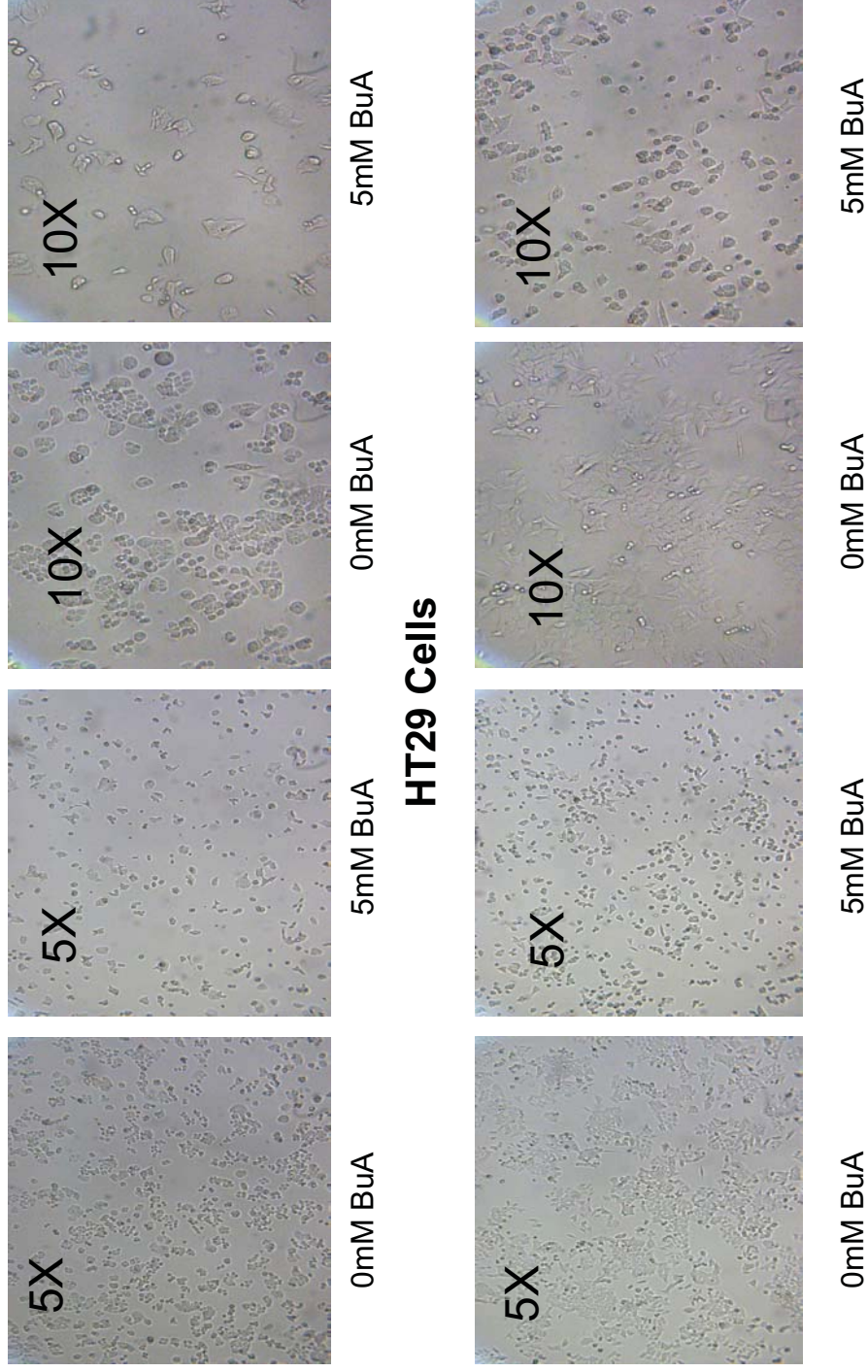


Figure 7.2: Representative photomicrographs of HT29 and HCT116 cells illustrating the changes in cell morphology induced by BuA exposure for 48 hours.

Shown are different magnitudes of untreated and BuA-treated cells.

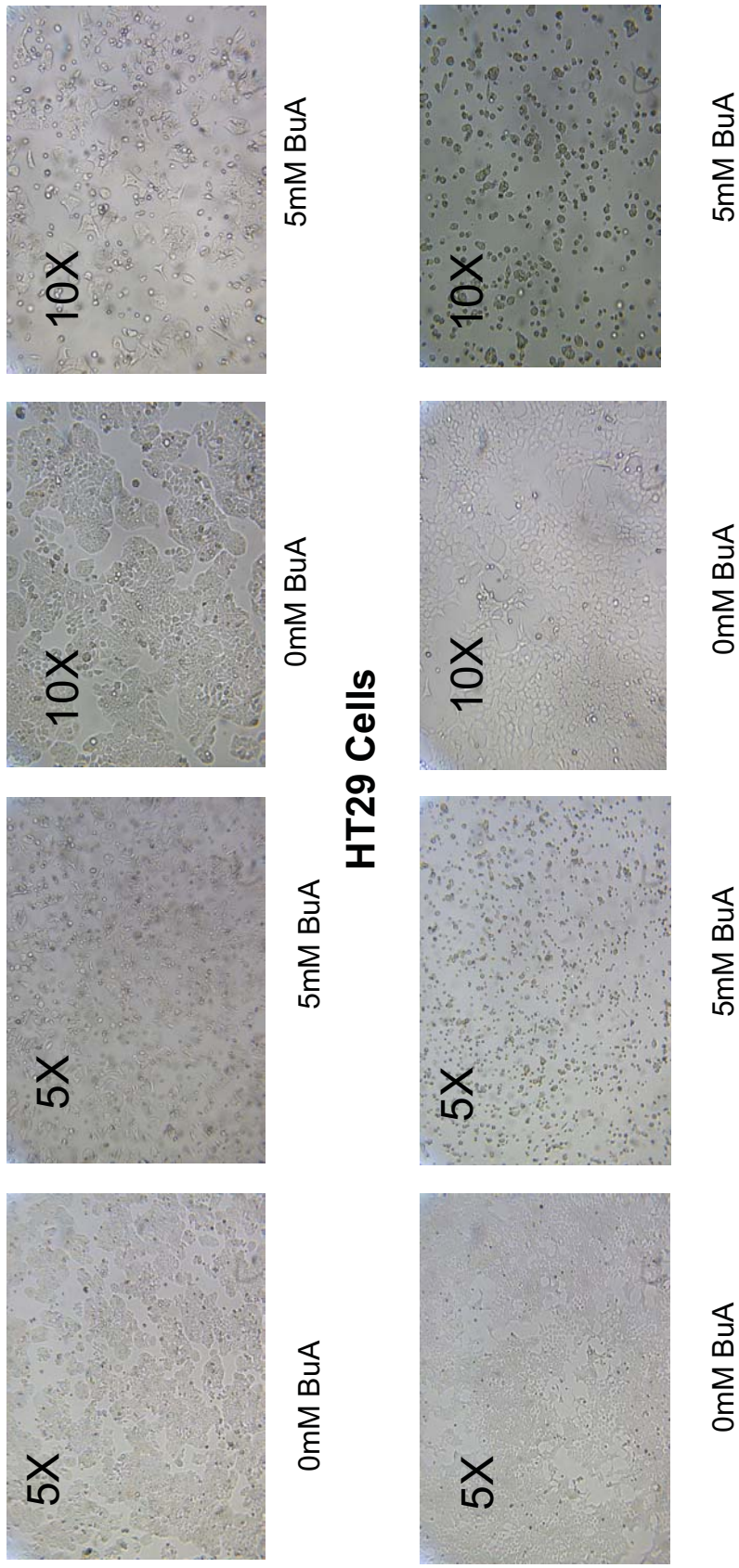


Figure 7.3a: Representative photomicrographs of HT29 cells illustrating the changes in cell morphology induced by BuA exposure and high and low glucose concentrations for 24 hours.

Shown are different magnitudes of untreated and BuA-treated cells.

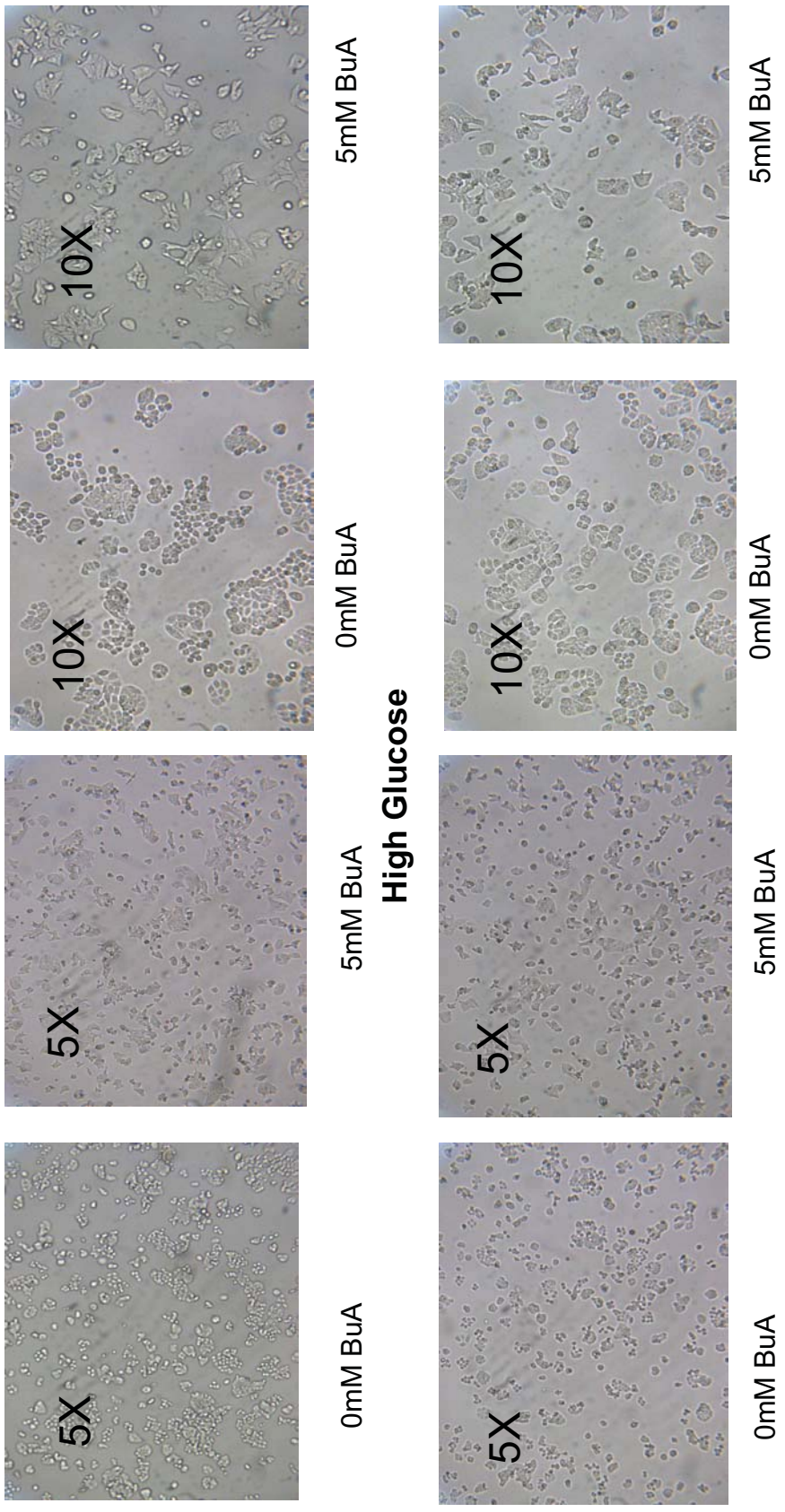


Figure 7.3b: Representative photomicrographs of HT29 cells illustrating the changes in cell morphology induced by BuA exposure and high and low glucose concentrations for 48 hours.

Shown are different magnitudes of untreated and BuA-treated cells.

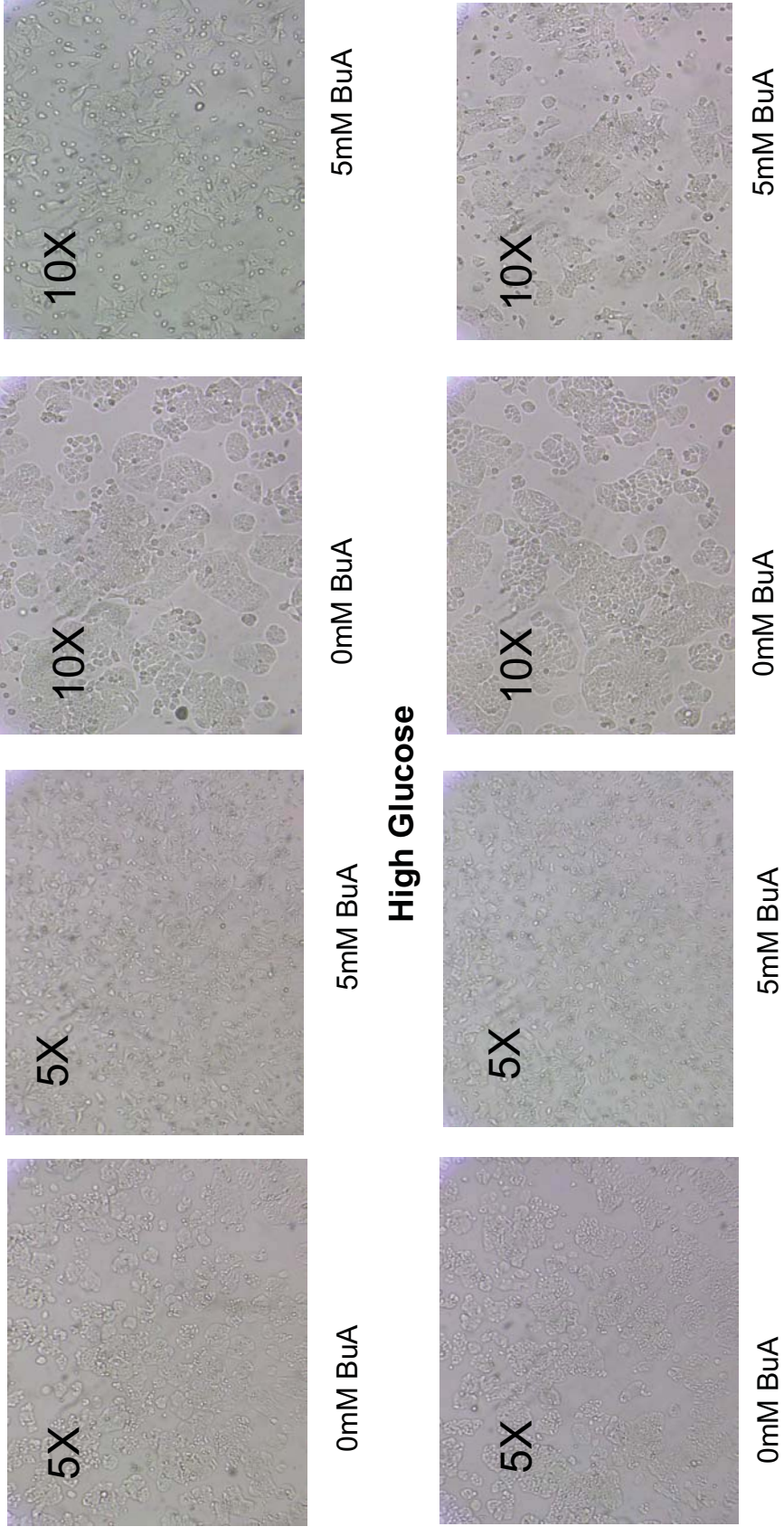
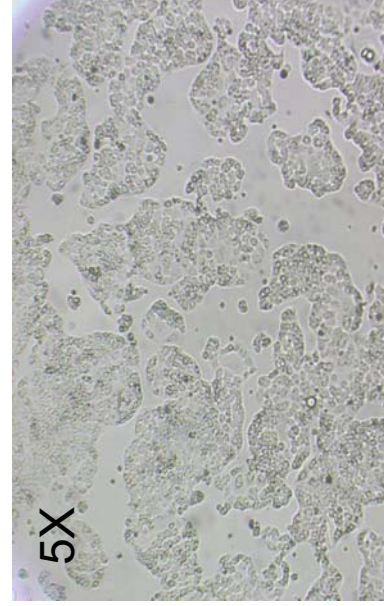
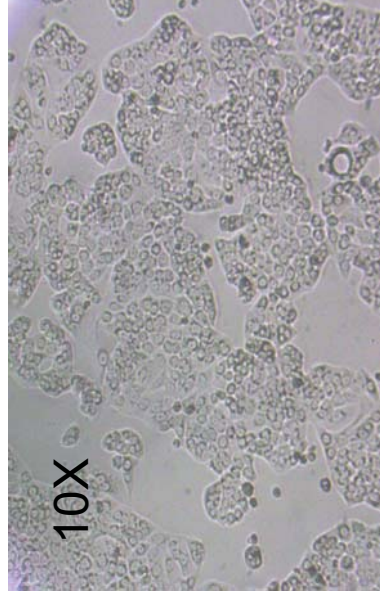


Figure 7.4: A representative photomicrograph illustrating the cell morphology of HT29-R cells grown in the presence of high and low glucose media.

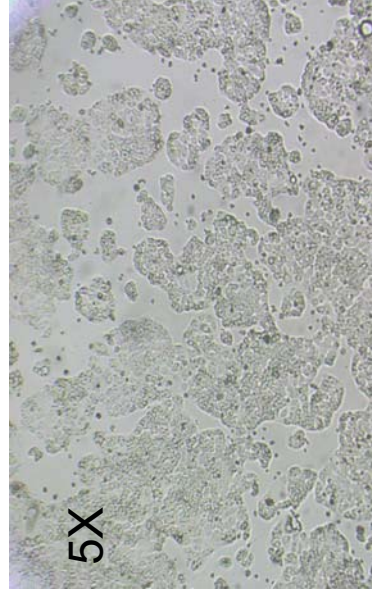
Shown are different magnifications of cells in high and low glucose media.



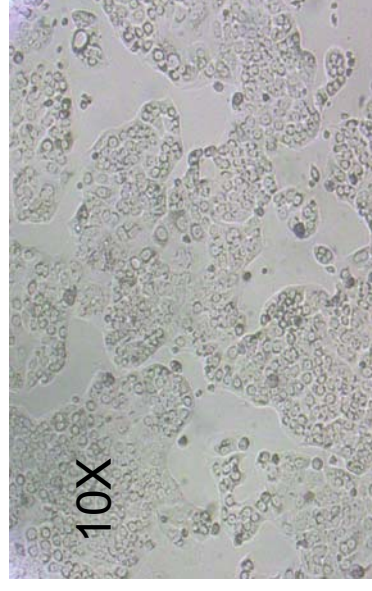
High Glucose



High Glucose



Low Glucose



Low Glucose

Figure 7.5

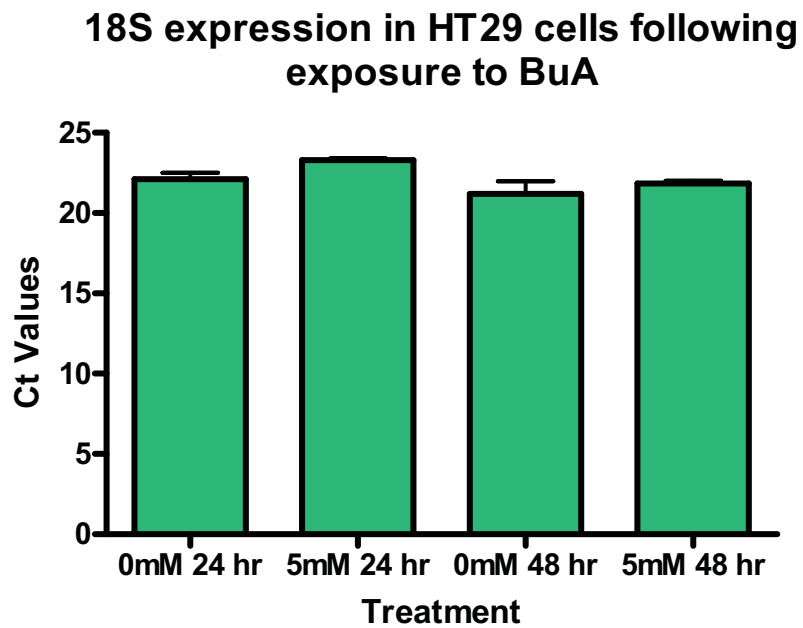
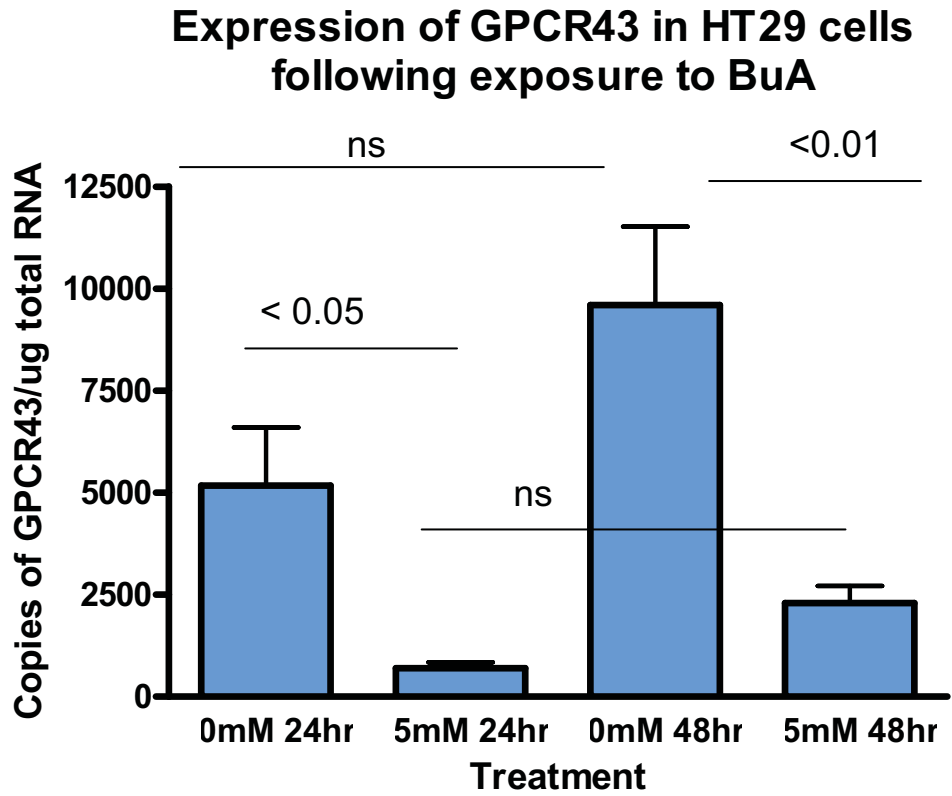


Figure 7.5: GPCR43 and 18S gene expression of HT29 cells following exposure to BuA for 24 or 48 hours.

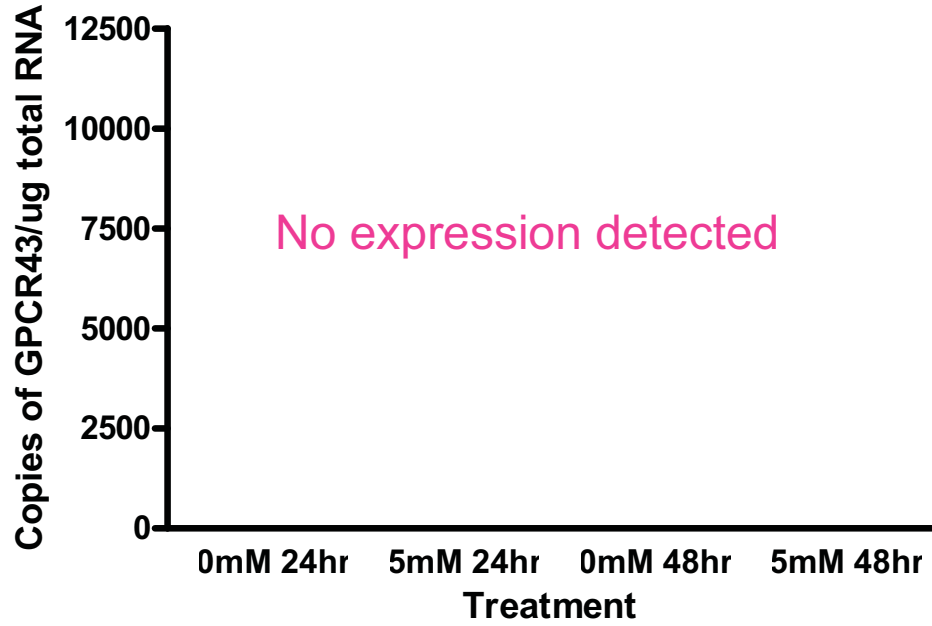
Expression of GPCR43 (a) or 18S (b) in HT29 cells grown in media alone or supplemented with BuA. Results show a reduced GPCR43 expression following BuA exposure for 24 and 48 hours, whilst 18S expression remained constant. Shown are the mean values \pm SEM.

Significance was determined using One-Way ANOVAs were performed with Tukey's post hoc testing and significance is indicated by values $p < 0.05$.

ns indicates not significantly different.

Figure 7.6

Expression of GPCR43 in HCT116 cells following exposure to BuA



18S expression in HCT116 cells following exposure to BuA

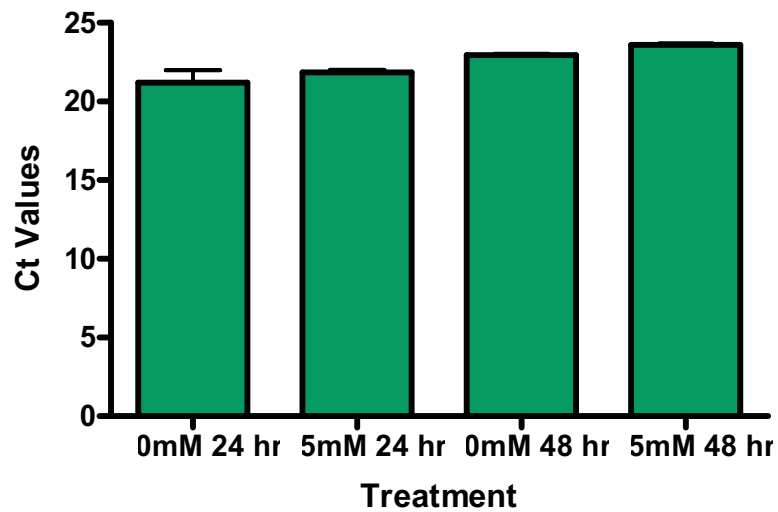


Figure 7.6: GPCR43 and 18S gene expression of HCT116 cells following exposure to BuA for 24 or 48 hours.

Expression of GPCR43 (a) or 18S (b) in HCT116 cells grown in media alone or supplemented with BuA. Results show GPCR43 expression was not detected in any treatment group, however 18S showed consistent expression. Shown are the mean values \pm SEM.

Significance was determined using One-Way ANOVAs were performed with Tukey's post hoc testing and significance is indicated by values $p < 0.05$.

ns indicates not significantly different.

GPCR43 expression in HT29 cells following exposure to BuA and altered glucose concentrations

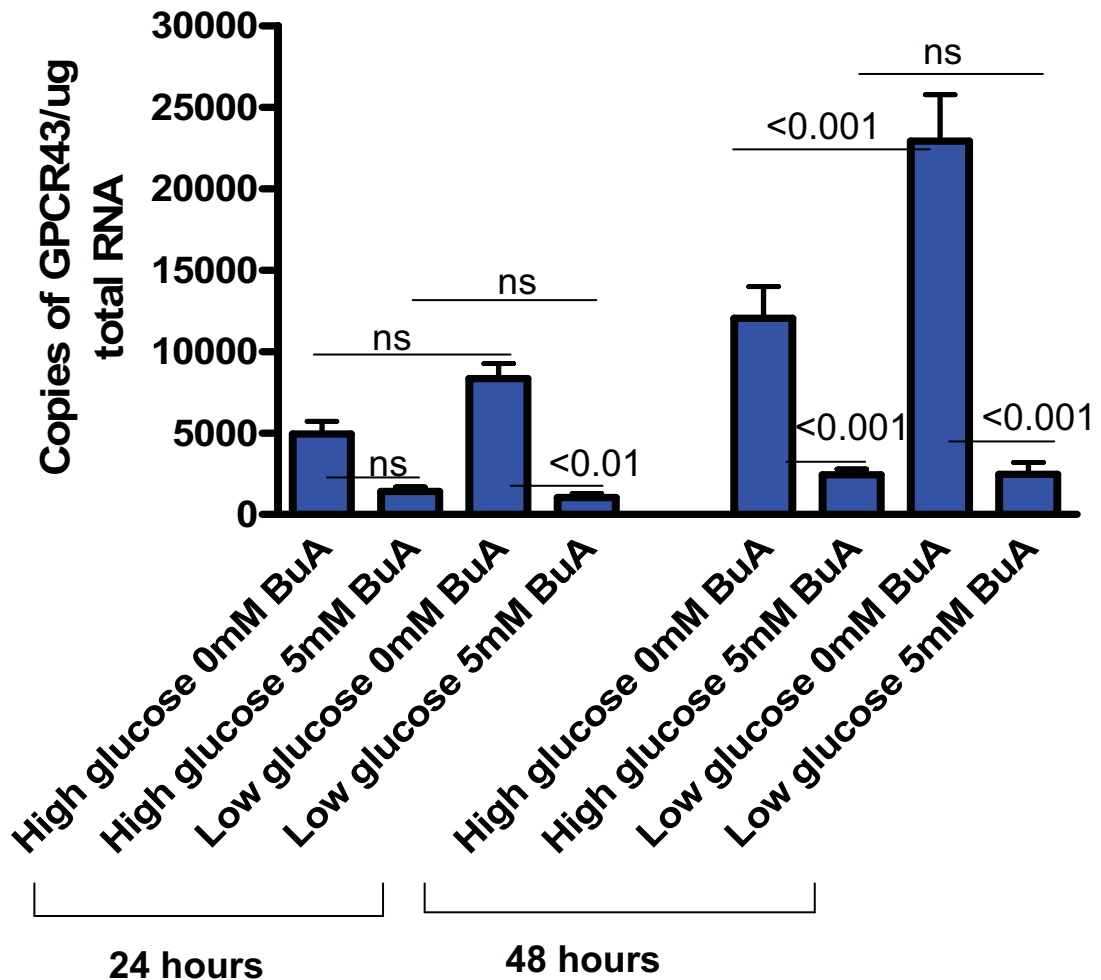


Figure 7.7: The influence of high and low glucose exposure for 24 and 48 hours on BuA mediated changes to GPCR43 expression in HT29 cells.

Results show a reduced GPCR43 receptor expression irrespective of glucose concentration. A significant difference in the GPCR43 expression was also detected in HT29 cells grown in low glucose media compared with high glucose media in the absence of BuA.

Shown are the mean values \pm SEM. Significance was determined using One-Way ANOVAs were performed with Tukey's post hoc testing and significance is indicated by values $p < 0.05$. ns indicates no significant differences were detected.

18S expression in HT29 cells following exposure to BuA and high or low glucose media

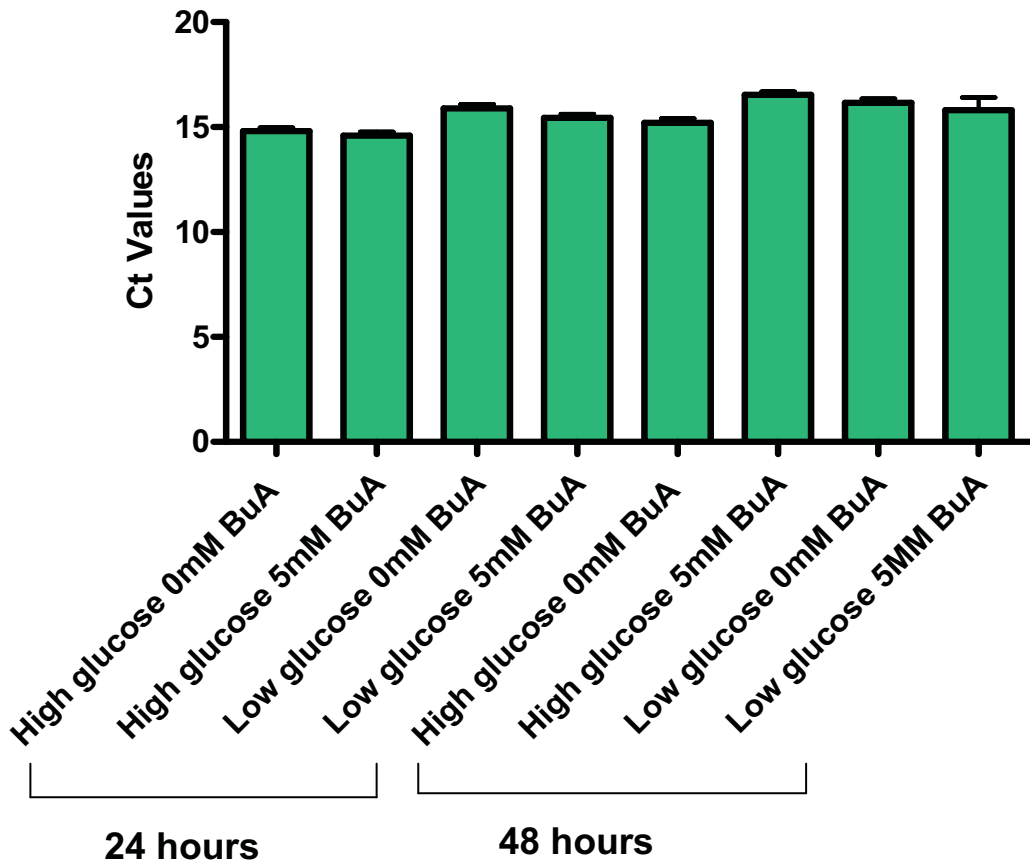
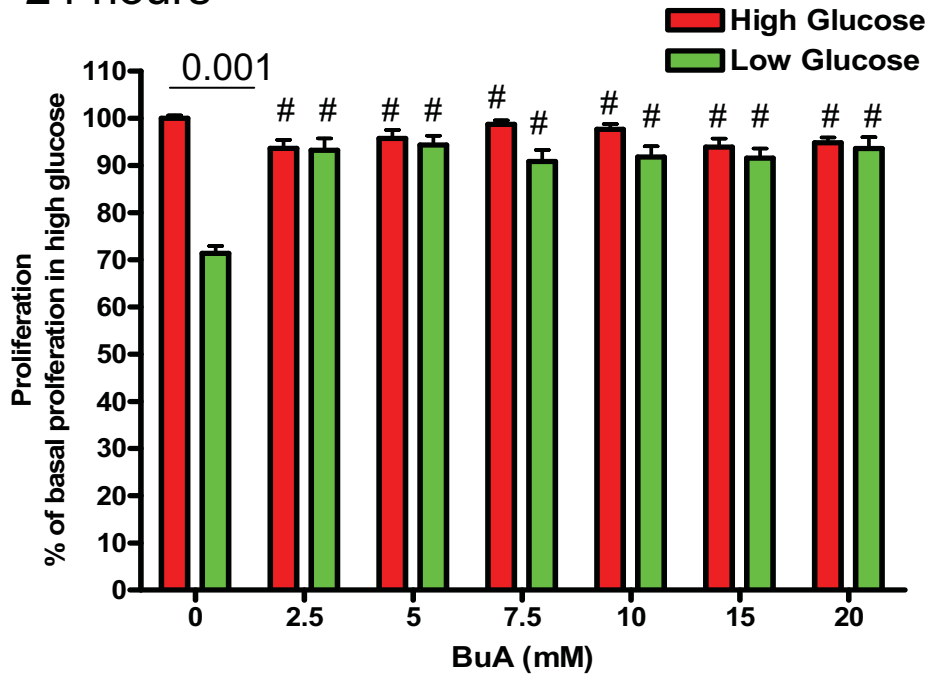


Figure 7.8: The constant expression of 18S in HT29 cells following exposure to BuA and high and low glucose concentrations for 24 and 48 hours.

Results show a consistent expression of 18S across all treatment groups. The mean values \pm SEM have been presented.

Figure 7.9

Proliferation of HT29 cells following exposure to BuA in the presence of high and low glucose media
24 hours



48 hours

Proliferation of HT29 cells following exposure to BuA in the presence of high and low glucose media

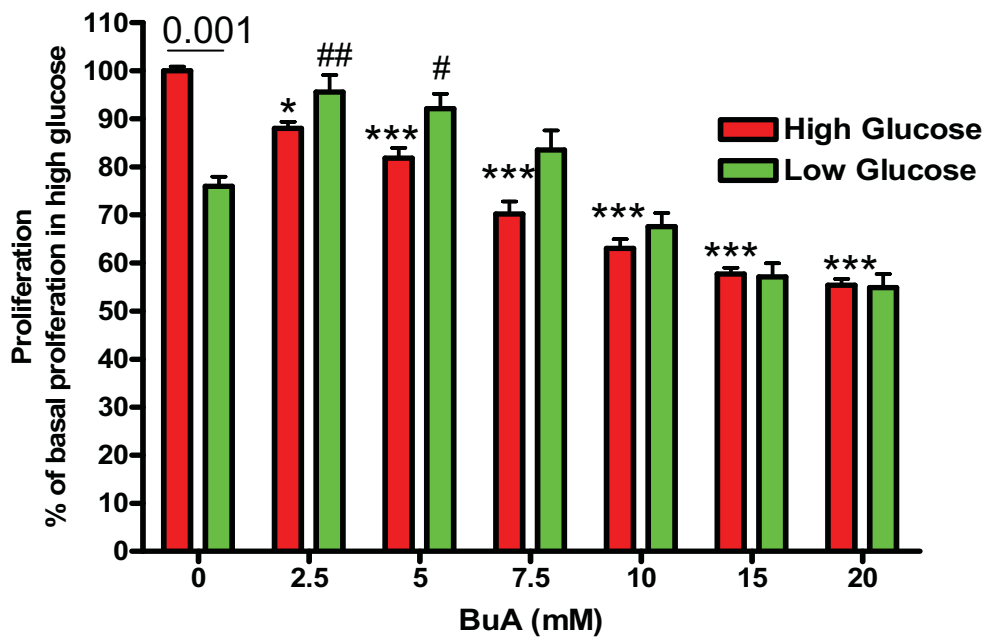


Figure 7.9: The influence of varying BuA concentrations on HT29 cell proliferation in the presence of high or low glucose media.

The results highlight the following:

- a) A significant decrease in the proliferation of HT29 cells grown in low glucose media for 24 and 48 hours in the absence of BuA.
- b) Little difference between the proliferation of HT29 cells in the high and low glucose treatments at 24 hours across the BuA concentrations.
- c) Significant increase in proliferation of HT29 cells grown in low glucose media compared with high glucose media for 48 hours at low BuA concentrations.

Each assay was conducted in triplicate with 3 replicates, with the mean values \pm SEM presented. Statistical analysis was conducted using One-way ANOVA with Tukey's post-hoc testing.

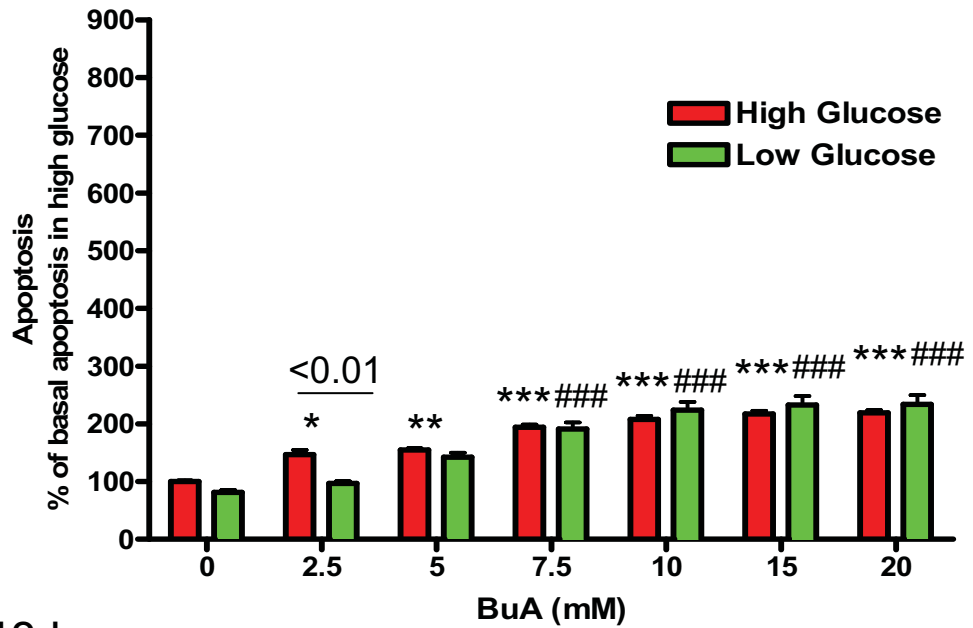
(*) $p < 0.05$ (**) $p < 0.01$ (***) $p < 0.001$ denotes significance compared to 0mM BuA alone in high glucose media.

(#) $p < 0.05$ (##) $p < 0.01$ (###) $p < 0.001$ denotes significance compared to 0mM BuA alone in low glucose media.

Figure 7.10

24 hours

Apoptosis of HT29 cells following exposure to BuA in the presence of high and low glucose



48 hours

Apoptosis of HT29 cells following exposure to BuA in the presence of high and low glucose media

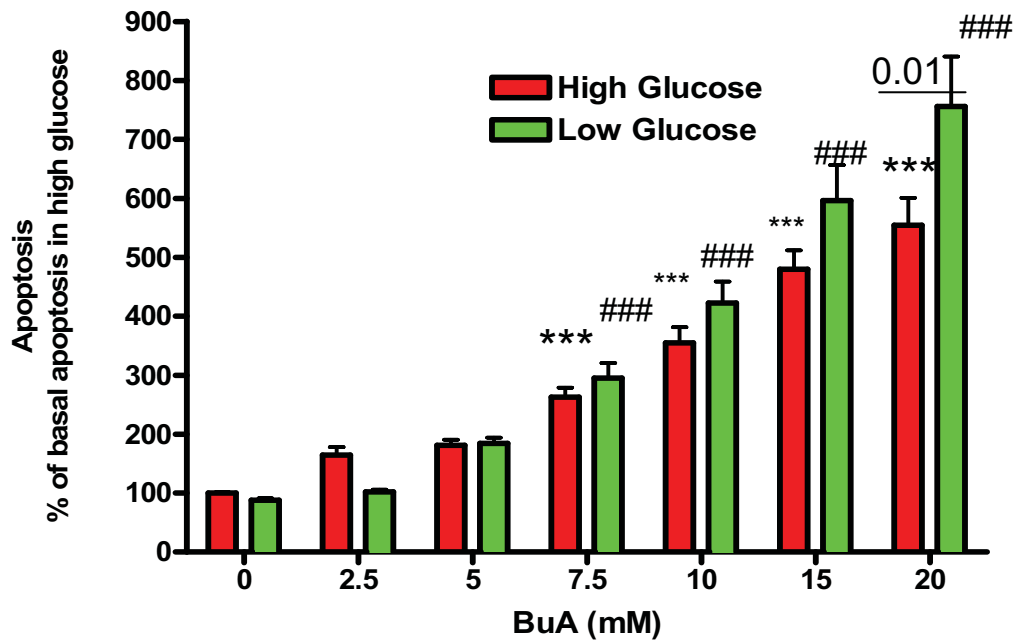


Figure 7.10: The influence of varying BuA concentrations on HT29 cell apoptosis in the presence of high or low glucose media.

The results highlight the following:

- a) Little difference between the apoptosis of HT29 cells in the high and low glucose treatments at 24 and 48 hours across the BuA concentrations.

- b) Significant differences between the apoptosis induced in high and low glucose media were observed only at 2.5mM BuA after 24 hours and 20mM BuA after 48 hours.

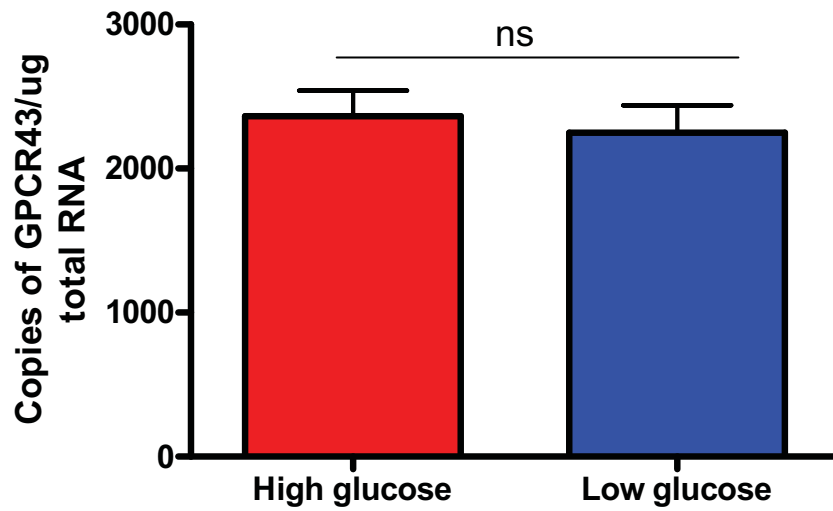
Each assay was conducted in triplicate with 3 replicates, with the mean values \pm SEM presented. Statistical analysis was conducted using One-way ANOVA with Tukey's post-hoc testing.

(*) $p < 0.05$ (**) $p < 0.01$ (***) $p < 0.001$ denotes significance compared to 0mM BuA alone in high glucose media.

(#) $p < 0.05$ (##) $p < 0.01$ (###) $p < 0.001$ denotes significance compared to 0mM BuA alone in low glucose media.

Figure 7.11

a **Expression of GPCR43 in HT29-R cells grown in high or low glucose media**



b **18S expression in HT29-R Cells grown in high or low glucose media**



Figure 7.11: GPCR43 and 18S gene expression in HT29-R cells grown in media containing high or low glucose concentrations.

Panel (a) shows the expression of GPCR43 on HT29-R cells grown in high or low glucose media. No significant differences were observed between cells grown in either media.

Panel (b) shows uniform expression of 18S was observed in both treatment groups.

The mean values \pm SEM are presented. Significance was determined using One-Way ANOVAs were performed with Tukey's post hoc testing and significance is indicated by values $p < 0.05$. ns indicates no significant differences were detected.

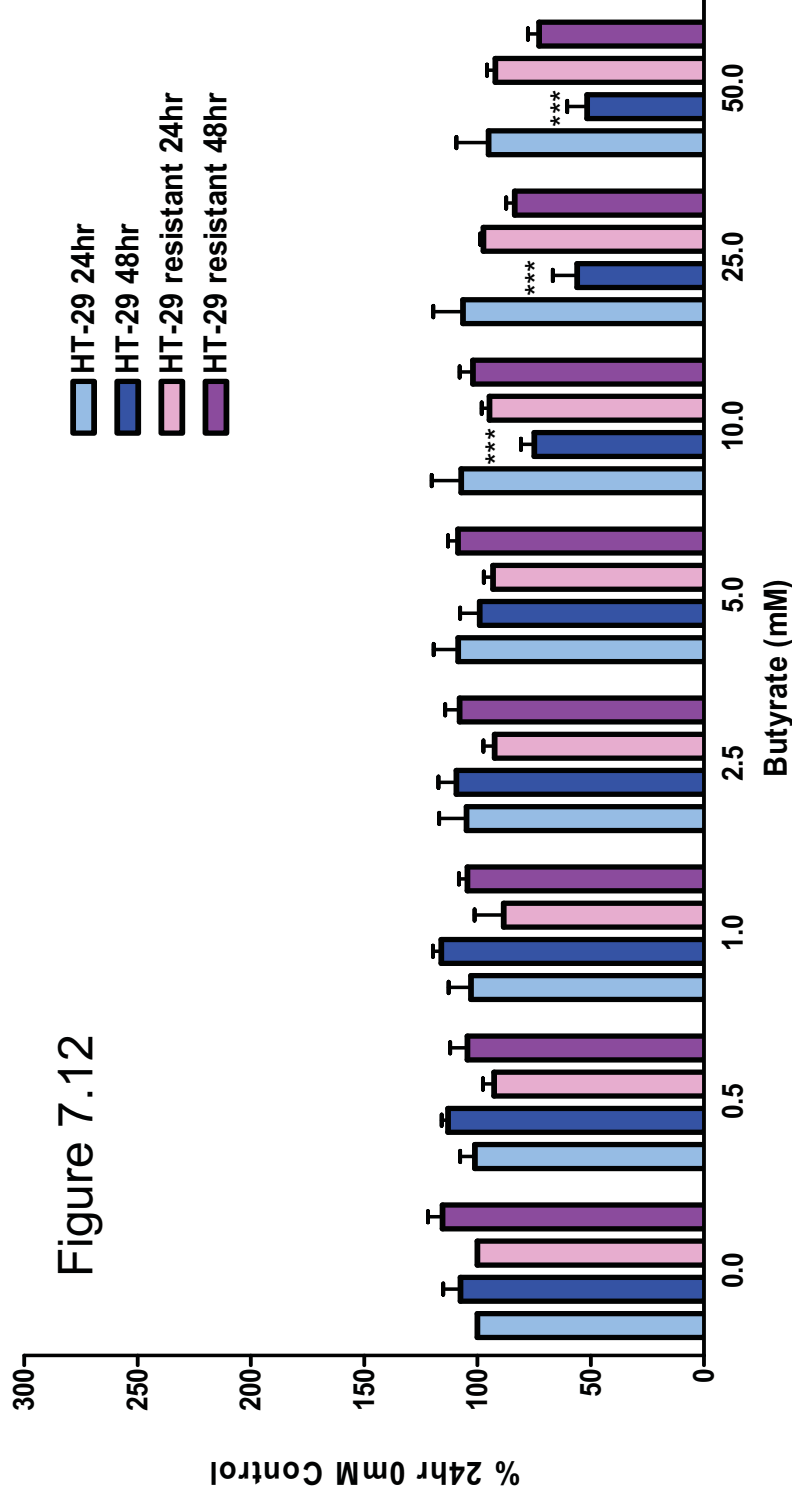


Figure 7.12: A comparison of the effect of varying BuA concentrations for 24 and 48 hours on HT29 and HT29-R cell proliferation.

Results show that whilst HT29 cells undergo BuA-induced decreases in proliferation, the HT29-R cells are not BuA-sensitive.

Each assay was conducted in triplicate with 4 replicates, with the mean \pm SEM shown. Statistical analysis was conducted using One-way ANOVA with Tukey's post-hoc testing. *p<0.05, **p<0.01, ***p<0.001 compared to 0mM control (1-way ANOVA with Tukey's Post-Hoc test).

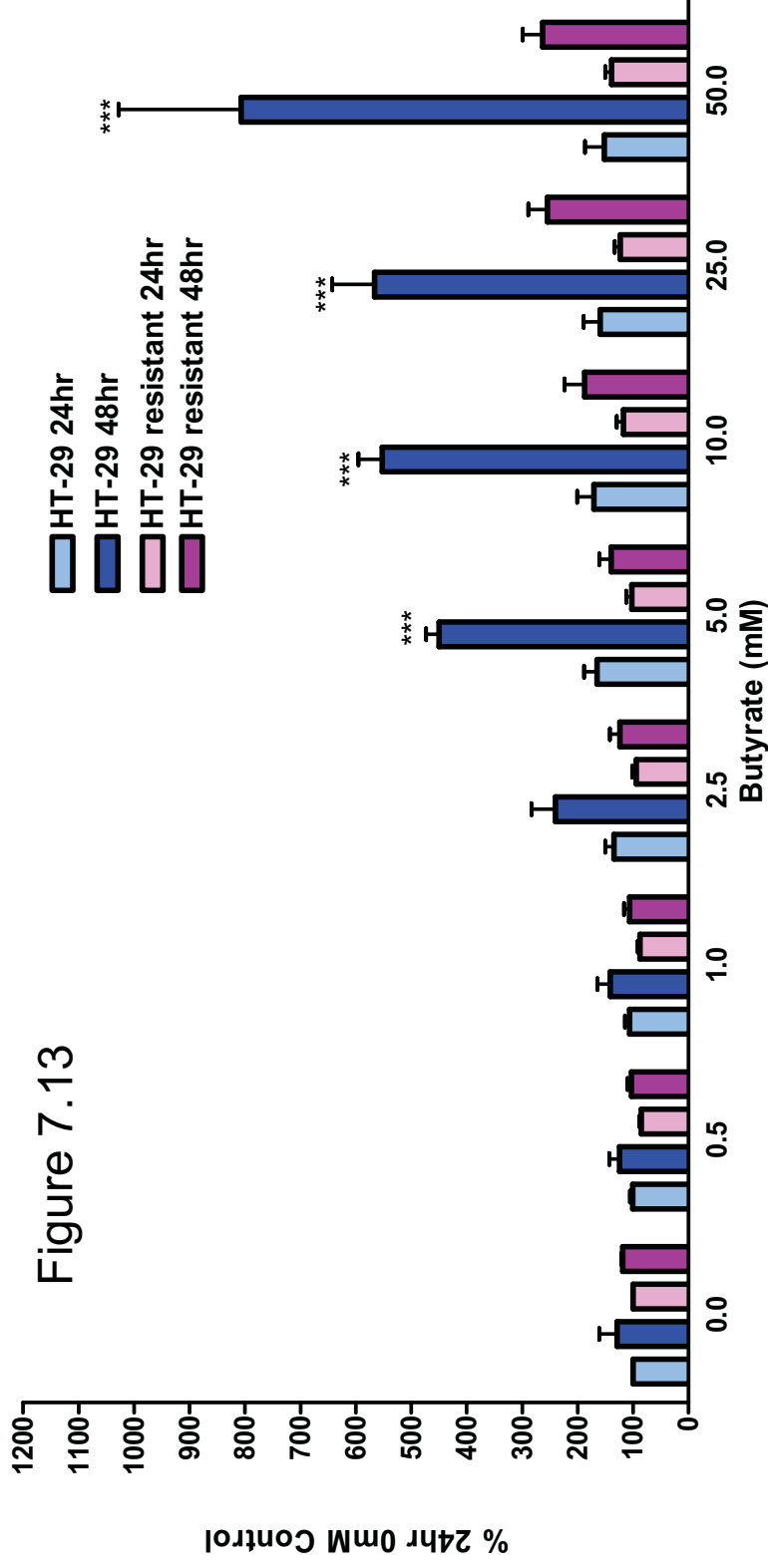


Figure 7.13: A comparison of the effect of varying BuA concentrations for 24 and 48 hours on HT29 and HT29-R cell apoptosis.

Results show that whilst HT29 cells undergo BuA-induced apoptosis, the HT29-R cells are not BuA-sensitive.

Each assay was conducted in triplicate with 4 replicates, with the mean \pm SEM shown. Statistical analysis was conducted using One-way ANOVA with Tukey's post-hoc testing. * $p < 0.05$, ** $p < 0.01$, *** $p < 0.001$ compared to 0mM control (1-way ANOVA with Tukey's Post-Hoc test).

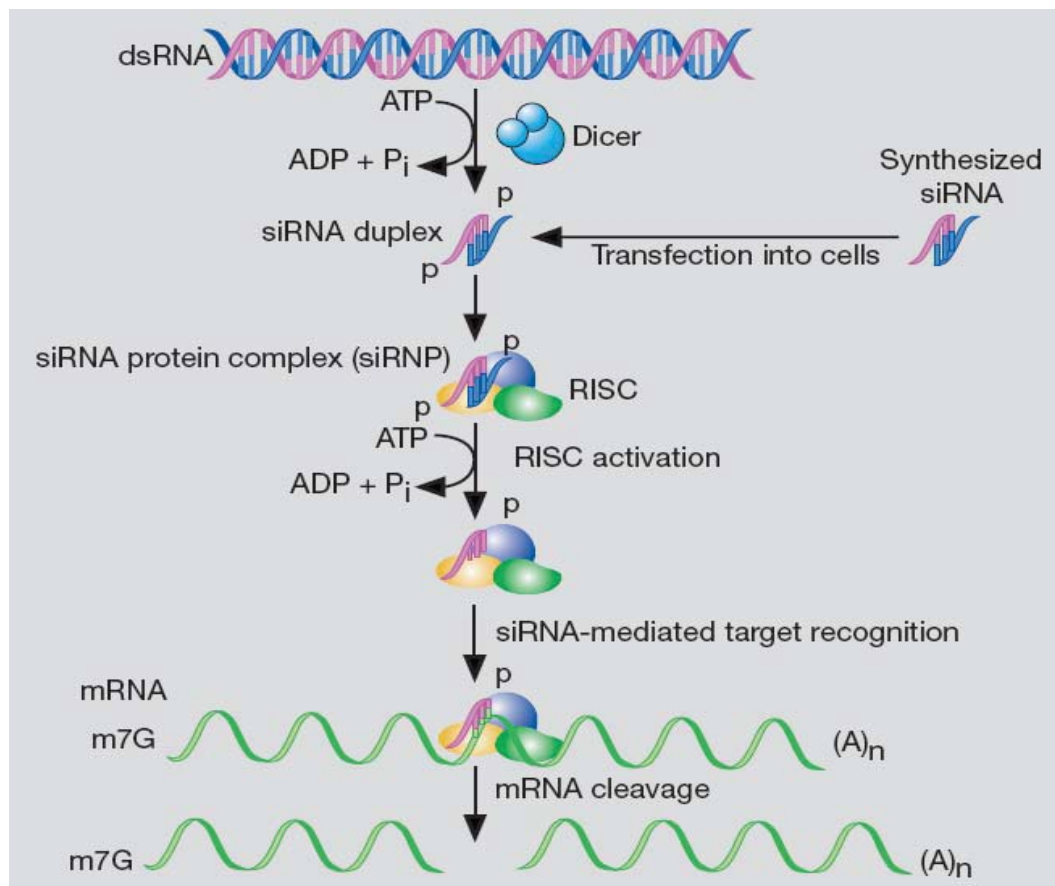


Figure 8.1: A schematic representation illustrating the RNAi pathway.

The diagram was reproduced from the Eppendorf Applications note 110, April 2005.

Cells visualised
without fluorescence
microscopy

Cells visualised
with fluorescence
microscopy

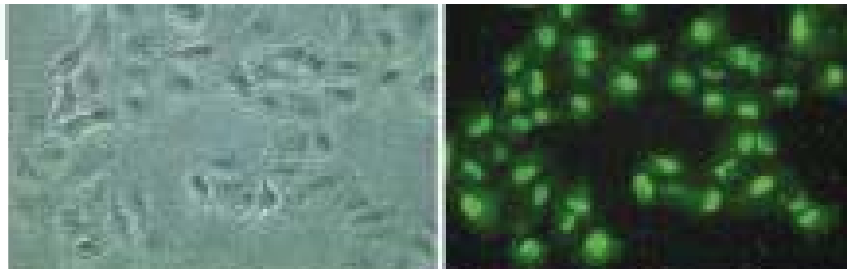


Figure 8.2: The manufacturer's example of a photomicrograph of cells fluorescing after successful transfection with Block-iT oligo.

Adapted from Invitrogen Block-iT Fluorescent Oligo Manual #137 50062 2013.

Knockdown of GPCR43 using siRNA at 24 hours

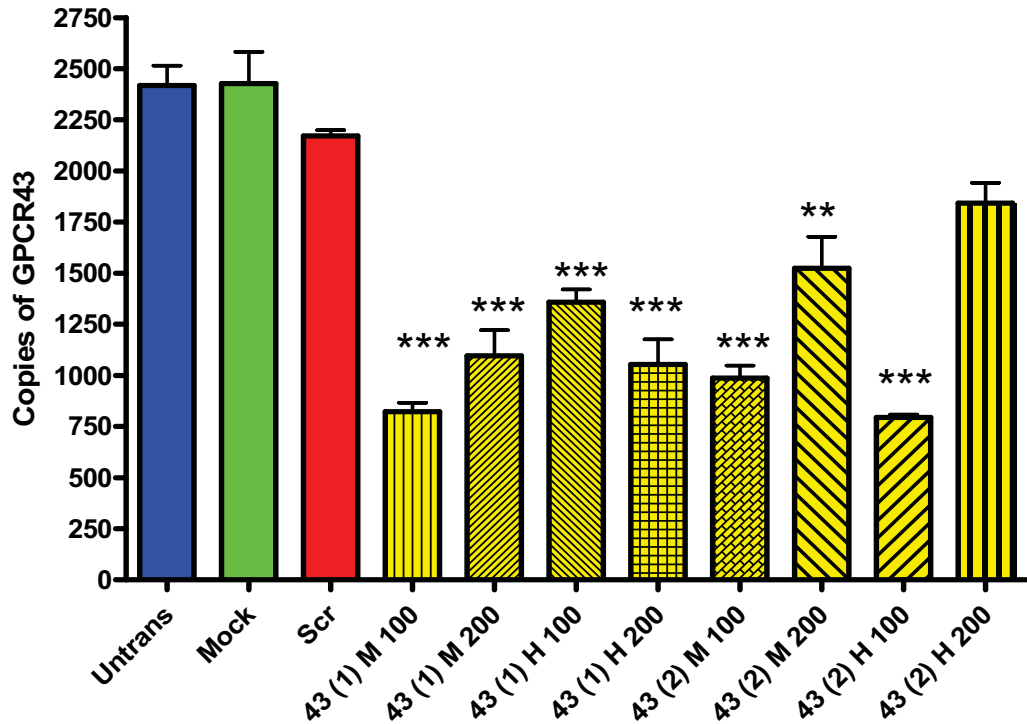


Figure 8.3: Knockdown of GPCR43 achieved after 24 hours using 2 siRNA oligos at different concentrations combined with 2 transfection reagent concentrations in HT29 cells.

The results show that most siRNA transfection combinations are sufficient to induce significant knockdown of GPCR43 compared to controls at this time point.

Shown are the mean values \pm SEM. Statistical analysis was conducted using One-way ANOVA with Tukey's post-hoc testing.

* $p < 0.05$, ** $p < 0.01$, *** $p < 0.001$ compared to untransfected control.

43 (1) = 1st siRNA

43(2) = 2nd siRNA

M= Mid concentration of transfection reagent

H= High concentration of transfection reagent

100 = 100nmole of siRNA

200 = 200nmole of siRNA

Knockdown of GPCR43 using siRNA after 48 hours

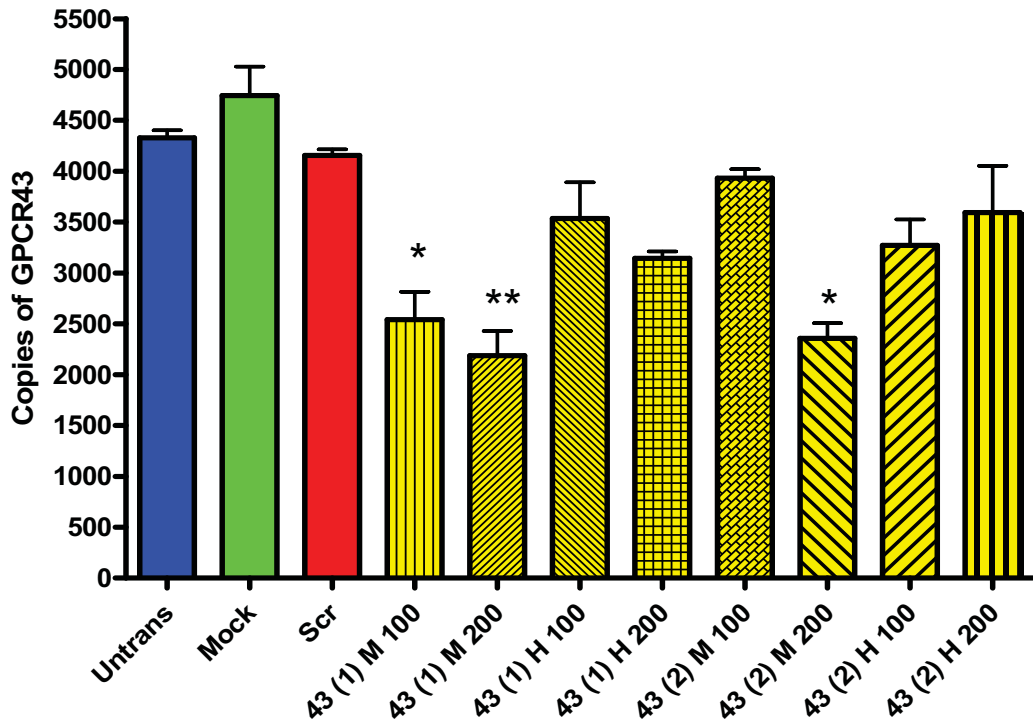


Figure 8.4: Knockdown of GPCR43 achieved after 48 hours using 2 siRNA oligos at different concentrations combined with 2 transfection reagent concentrations in HT29 cells.

The results show that some siRNA transfection combinations are sufficient to induce significant knockdown of GPCR43 compared to controls at this timepoint.

Shown are the mean values \pm SEM. Statistical analysis was conducted using One-way ANOVA with Tukey's post-hoc testing.

* $p < 0.05$, ** $p < 0.01$, *** $p < 0.001$ compared to untransfected control.

43 (1) = 1st siRNA

43(2) = 2nd siRNA

M= Mid concentration of transfection reagent

H= High concentration of transfection reagent

100 = 100nmole of siRNA

200 = 200nmole of siRNA

Expression of GPCR43 in cells treated with siRNA

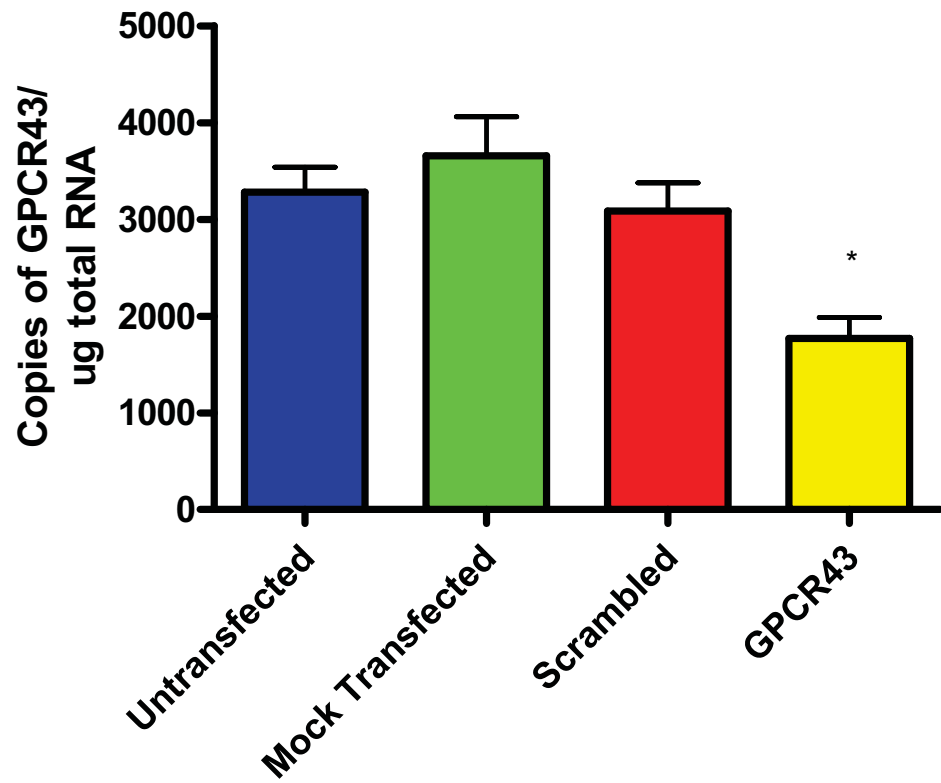


Figure 8.5: Expression of GPCR43 in HT29 cells used in proliferation and apoptosis assays following siRNA knockdown.

Results show that GPCR43 expression was significantly reduced by siRNA transfection compared with all controls.

Shown are the mean values \pm SEM. Statistical analysis was conducted using One-way ANOVA with Tukey's post-hoc testing.

* $p < 0.05$ compared to untransfected control.

18S expression in cells treated with siRNA

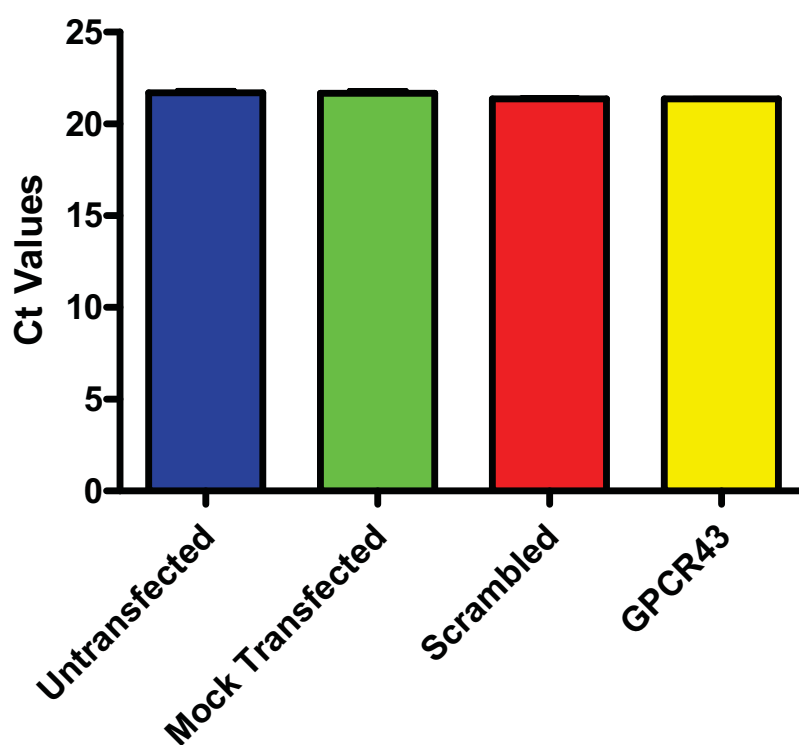


Figure 8.6: 18S expression in HT29 cells following siRNA transfection.

Results show even 18S expression is seen following exposure to different components of the siRNA transfection process. The mean values \pm SEM are presented.

Figure 8.7

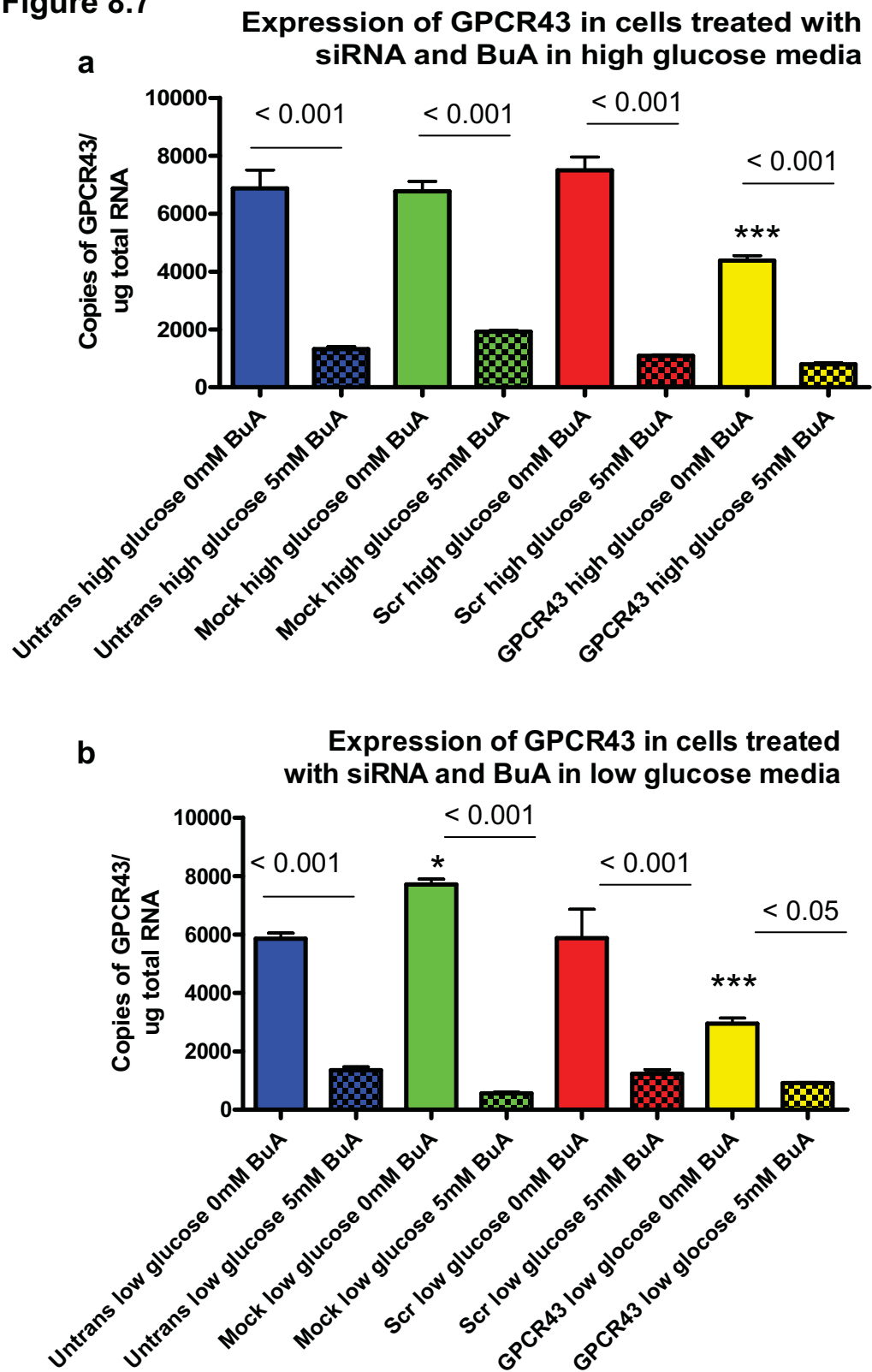


Figure 8.7: Expression of GPCR43 in HT29 cells following siRNA transfection and exposure to BuA in high and low glucose media.

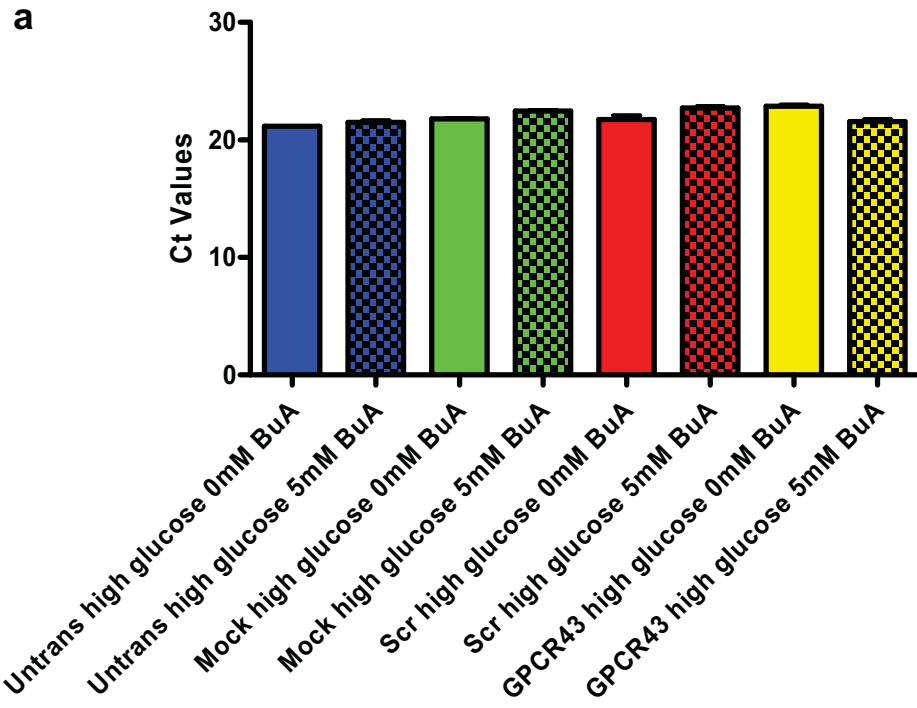
Results show a significant decrease in GPCR43 expression in all treatment groups, including controls, with the addition of BuA which is greater than the reduction in GPCR43 expression induced by siRNA transfection.

Shown are the mean values \pm SEM. Statistical analysis was conducted using One-way ANOVA with Tukey's post-hoc testing.

* $p < 0.05$, ** $p < 0.01$, *** $p < 0.001$ compared to the untransfected control.

Figure 8.8

Expression of 18S in cells treated with siRNA and BuA in high glucose media



18S expression in cells treated with siRNA and BuA in low glucose media

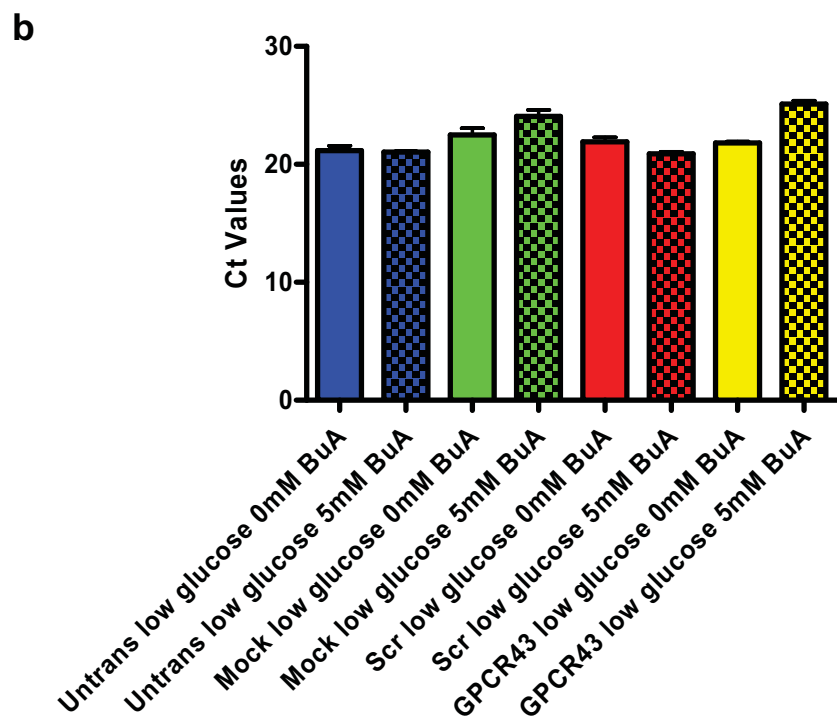


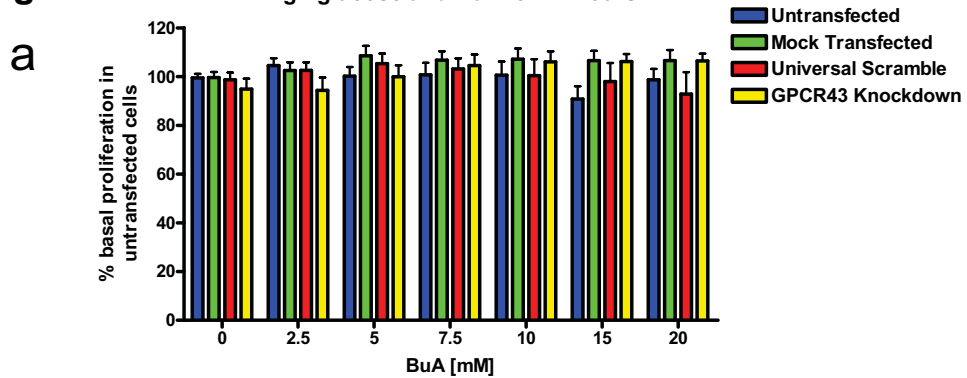
Figure 8.8: Expression of 18S in HT29 cells following siRNA transfection and exposure to BuA in high and low glucose media.

In contrast to Figure 8.7, the results show a mostly consistent expression of 18S in all treatment groups with the addition of BuA.

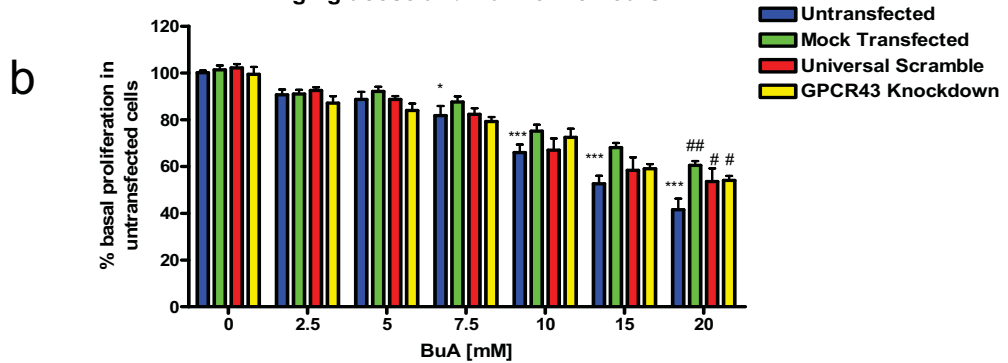
The results are presented as mean \pm SEM.

Figure 8.9

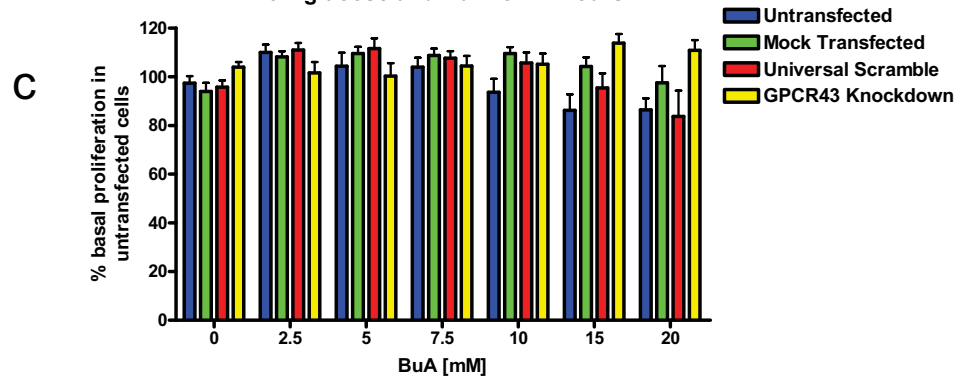
Proliferation of HT29 cells following exposure to high glucose and BuA for 24 hours



Proliferation of HT29 cells following exposure to high glucose and BuA for 48 hours



Proliferation of HT29 cells following exposure to low glucose and BuA for 24 hours



Proliferation of HT29 cells following exposure to low glucose and BuA for 48 hours

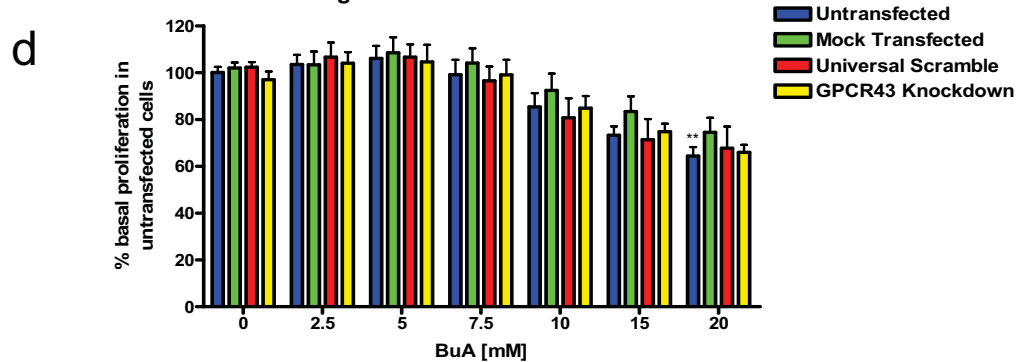


Figure 8.9: Effect of BuA on HT29 proliferation in high (a and b) or low glucose media (c and d) following siRNA treatment for 24 hours (a and c) and 48 hours (b and d).

Results show that GPCR43 knockdown did not significantly alter the BuA-induced proliferative response of HT29 cells compared to controls treated with transfection reagent and siRNA molecules.

The mean values \pm SEM have been presented. Statistical analysis was conducted using One-way ANOVA with Tukey's post-hoc testing.

* $p < 0.05$, ** $p < 0.01$, *** $p < 0.001$ compared to 0mM untransfected control.

$p < 0.05$, ## $p < 0.01$, ### $p < 0.001$ compared to 0mM untransfected control at the respective BuA concentration.

Figure 8.10 Apoptosis of HT29 cells following exposure to high glucose and BuA for 24 hours

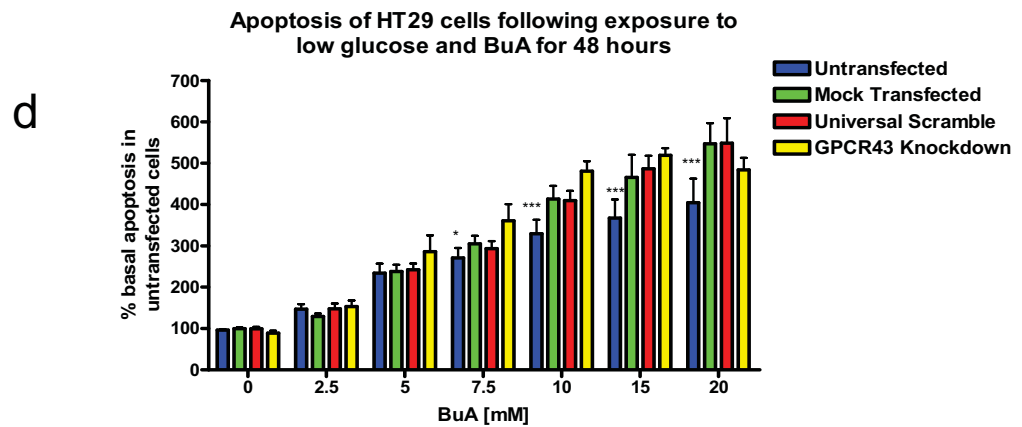
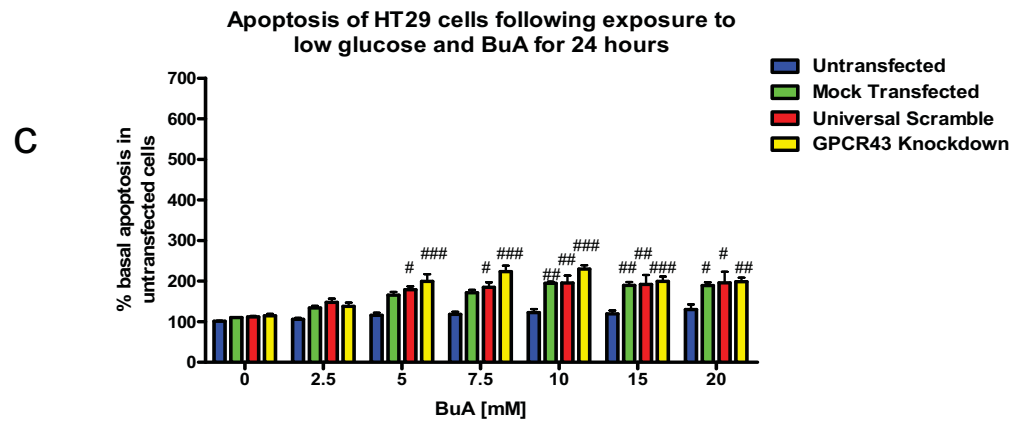
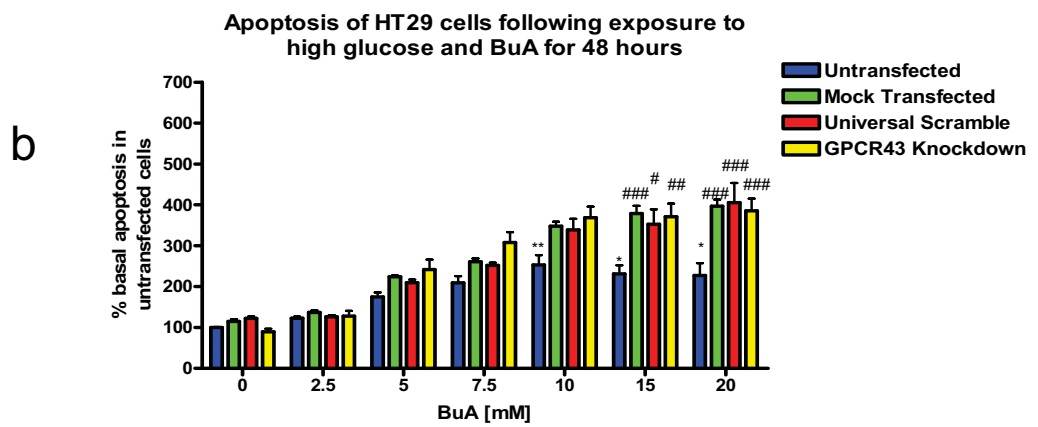
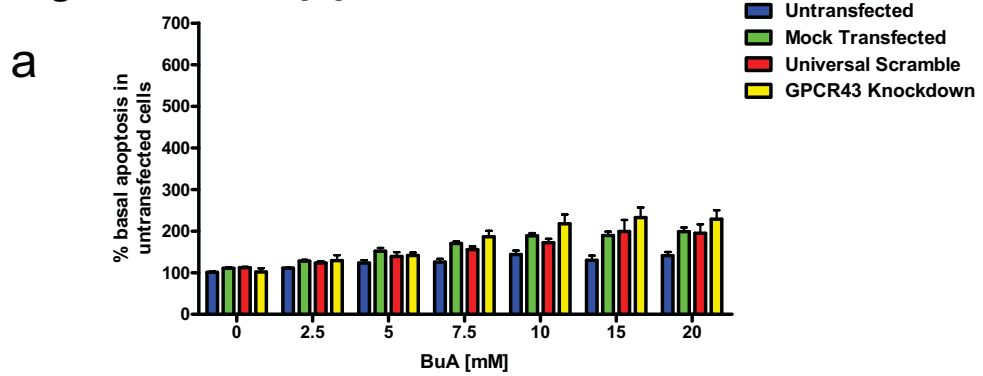


Figure 8.10: Effect of BuA on HT29 apoptosis in high (a and b) or low glucose media (c and d) following siRNA treatment for 24 hours (a and c) and 48 hours (b and d).

Results show that GPCR43 knockdown did not significantly alter the BuA-induced apoptotic response of HT29 cells compared to controls treated with transfection reagent and siRNA molecules.

The mean values \pm SEM have been presented. Statistical analysis was conducted using One-way ANOVA with Tukey's post-hoc testing.

* $p < 0.05$, ** $p < 0.01$, *** $p < 0.001$ compared to 0mM untransfected control.

$p < 0.05$, ## $p < 0.01$, ### $p < 0.001$ compared to 0mM untransfected control at the respective BuA concentration.

Normal		Tumour	
Number shown on Figure 9.4		Number shown on Figure 9.4	
		1	Dukes C, right colon
1	Dukes B, left colon	2	Dukes C, left colon
2	Dukes A, left colon	3	Dukes A, left colon, mucinous
3	normal mucosa, no cancer, patient received pre-operative radiotherapy	4	Dukes C, left colon
4	normal mucosa, no cancer	5	Dukes C, right colon, mucinous
5	Dukes C, mucinous adenocarcinoma, left colon	6	Dukes A, right colon
6	Dukes A, right colon	7	Dukes B, left colon, mucinous
7	Dukes C, Right colon	8	Adenoma, Right colon
8	Dukes B, Left colon	9	Dukes A, left colon
		10	Dukes C, left colon
		11	Dukes C, right colon, mucinous

Table 9.1: A summary of the staging of disease using Duke's methodology provided by Dr Andrew Ruszkiewicz.

Normal samples were taken from patients with normal mucosa or were samples of normal tissue taken from patients with cancer. For normal samples taken from patients with cancer the stage of the disease has been recorded in this table.

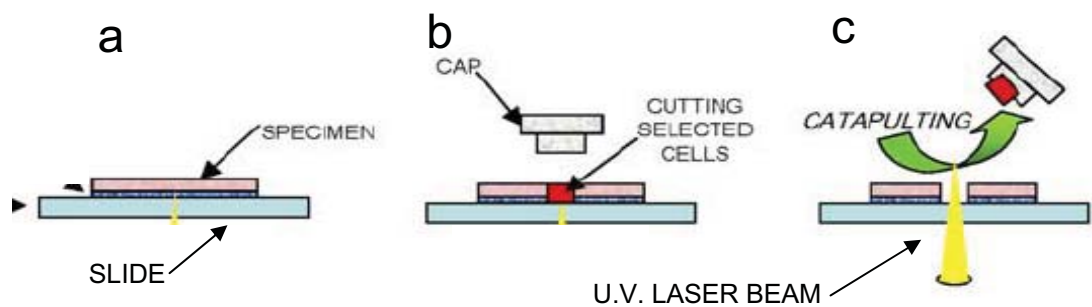


Figure 9.1 Pictorial representation demonstrating laser capture microscopy. Adapted from Pinzani et al 2006.

The procedure involves:

- (a) A slide containing the tissue specimen being placed on microscope stage.
- (b) The cap of the 0.5ml tube containing RNAlater being placed above the tissue section and cells of interest are selected using computer software.
- (c) The laser cutting the selected cells and catapults the section of tissue into the cap of the 0.5ml tube.

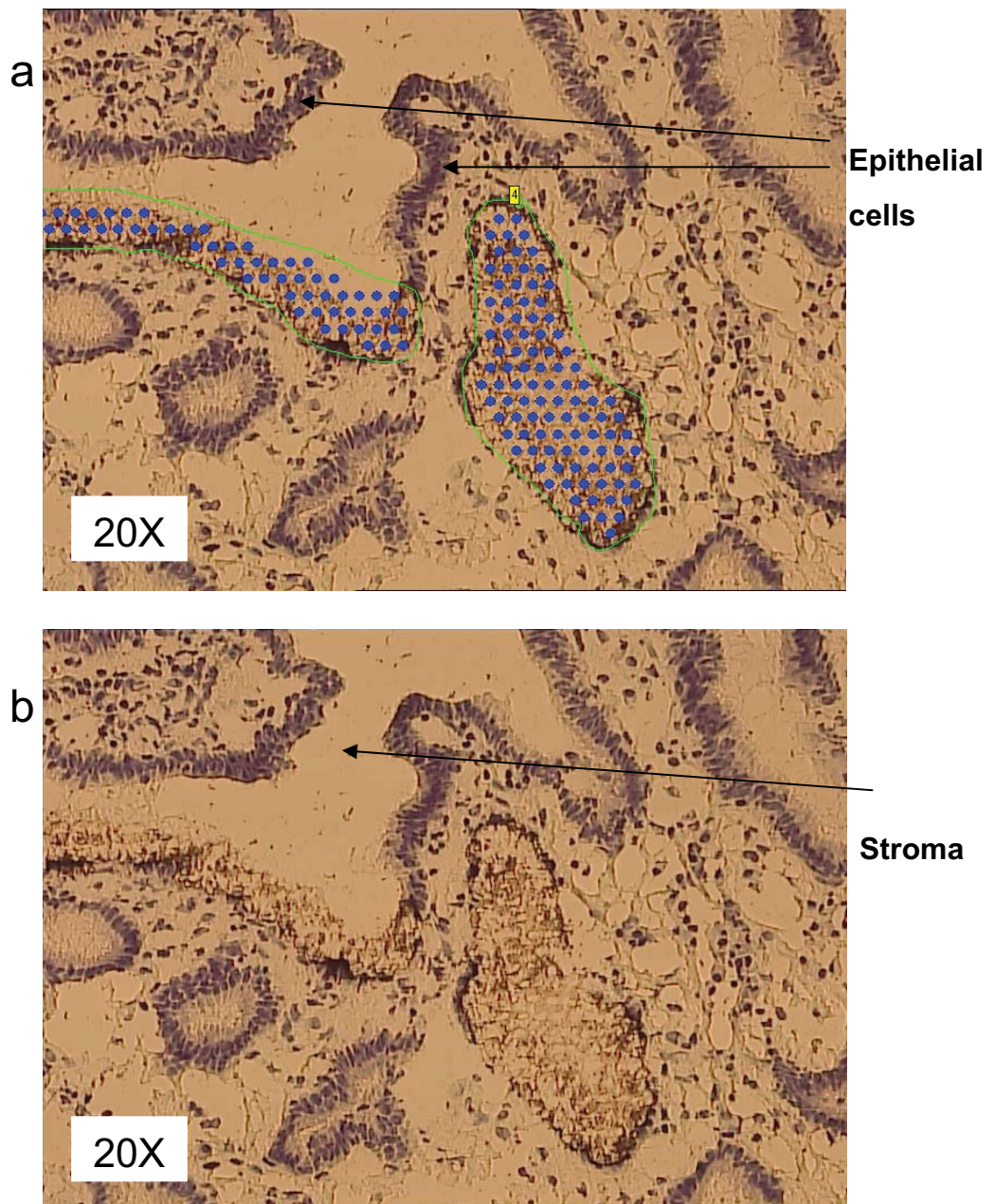


Figure 9.2: A representative photomicrograph of CRC tissue section taken using laser capture microdissection software at 20X magnification.

- (a) Tissue slide prior to dissection. Green lines surrounding the epithelium and blue dots indicate the section selected for the laser to dissect.
- (b) Shows the section of epithelium removed after laser dissection.

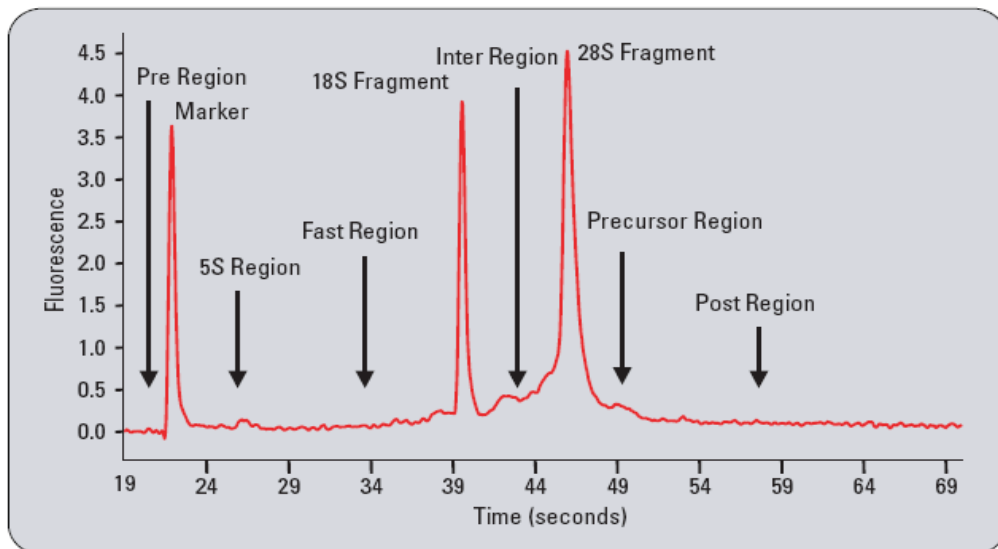


Figure 9.3: An electropherogram with details of regions indicative of RNA integrity.

Reproduced from Agilent Application note (RNA Integrity Number (RIN) – Standardization of RNA Quality Control).

Sample ID	ng/ul	260/280
Normal 1	262.28	2.04
Normal 2	1119.53	2.04
Normal 3	652.03	2.01
Normal 4	3127.59	1.99
Normal 5	1112.35	2.02
Normal 6	637.8	2.02
Normal 7	1886.04	2.01
Normal 8	211.94	1.91
CRC 1	No RNA detected	
CRC 2	675.7	1.99
CRC 3	99.84	2.01
CRC 4	No RNA detected	
CRC 5	629.12	2.02
CRC 6	1573.7	2.01
CRC 7	750.87	2.00
CRC 8	848.15	2.22
CRC 9	172.66	1.79
CRC 10	259.55	2.04
CRC 11	104.92	2.16

Table 9.2: A summary of the quality and quantity of RNA extracted from patient samples using the NanoDrop procedure.

Note: An absorbance ratio at 260:280nm of greater than 1.8 indicates RNA of good quality.

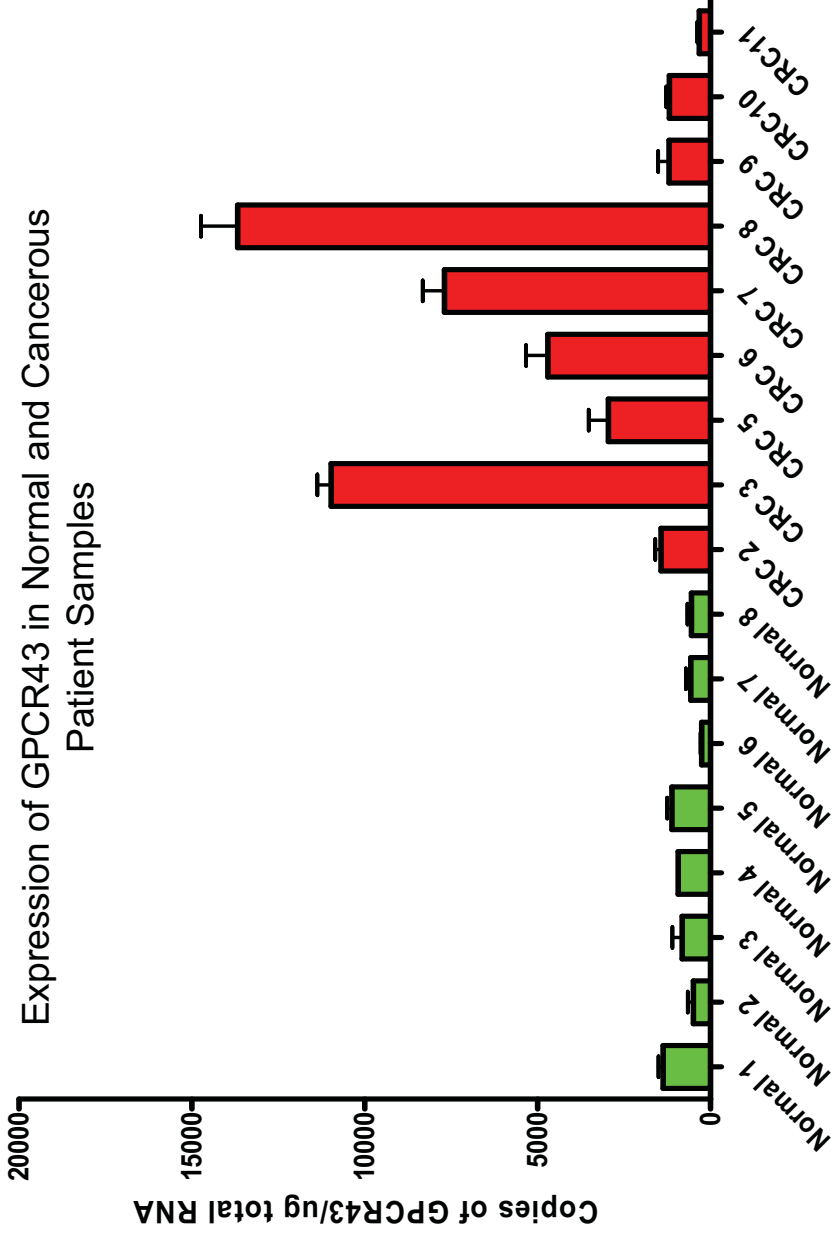


Figure 9.4: Expression of GPCR43 in patient samples.

Expression of GPCR43 in human normal and cancerous colon samples using Q-PCR and absolute quantitation. Shown are the mean values \pm SEM.

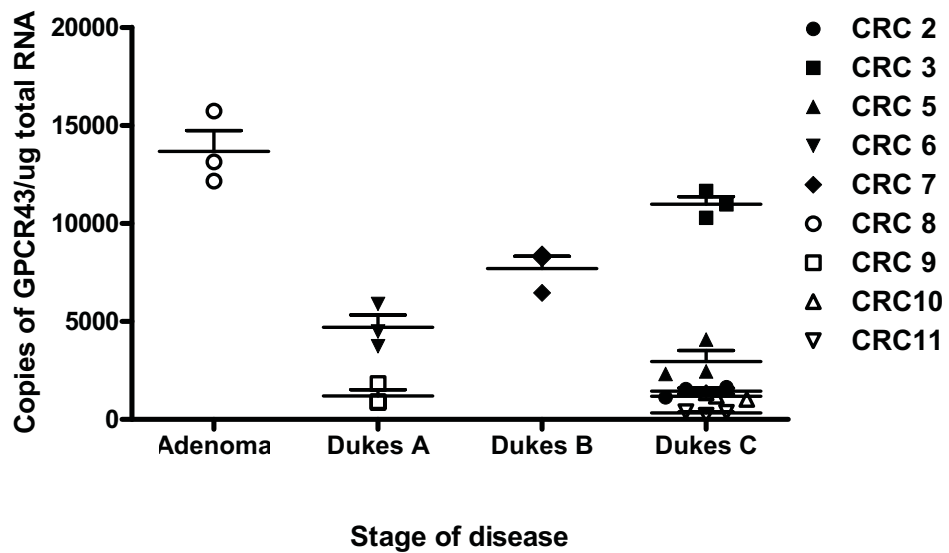


Figure 9.5: Comparison between the expression of GPCR43 and stage of CRC using Dukes staging.

The expression of GPCR43 from each patient analysed using Q-PCR was plotted against the stage of disease to determine if a correlation between GPCR43 expression and progression of CRC existed.

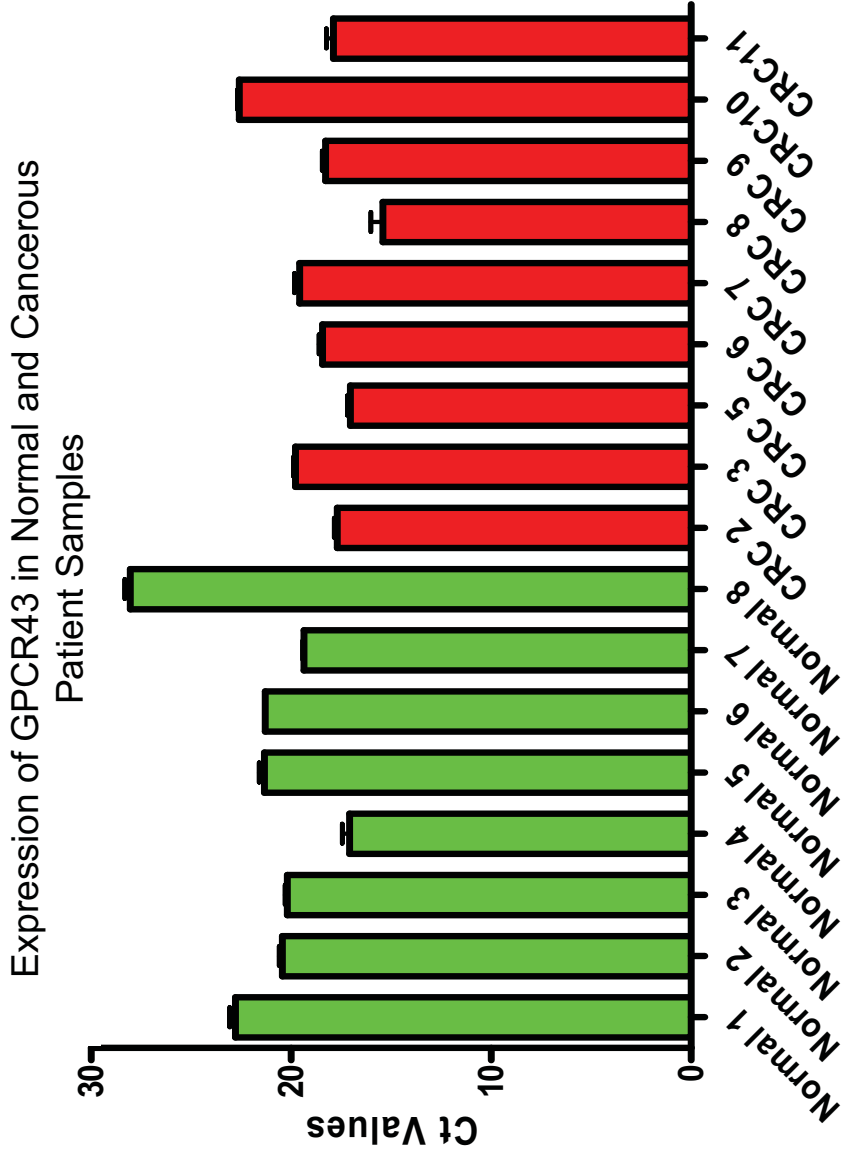


Figure 9.6: 18S expression in normal and cancerous patient samples.

Expression of 18S in patient normal and cancerous colon samples remained fairly constant, especially compared with the differences observed in GPCR43 expression shown in Figure 9.4. Shown are the mean values \pm SEM.

Sample ID	ng/ul	A260/280
CRC 3	14.32	1.37
CRC 5	-56.68	1.96
CRC 8	91.94	-10.08
CRC10	76.82	-4.26

Table 9.3: A summary of the quality and quantity of RNA extracted from laser dissected patient samples using the NanoDrop procedure.

Note: An absorbance ratio at 260:280nm of greater than 1.8 indicates RNA of good quality.

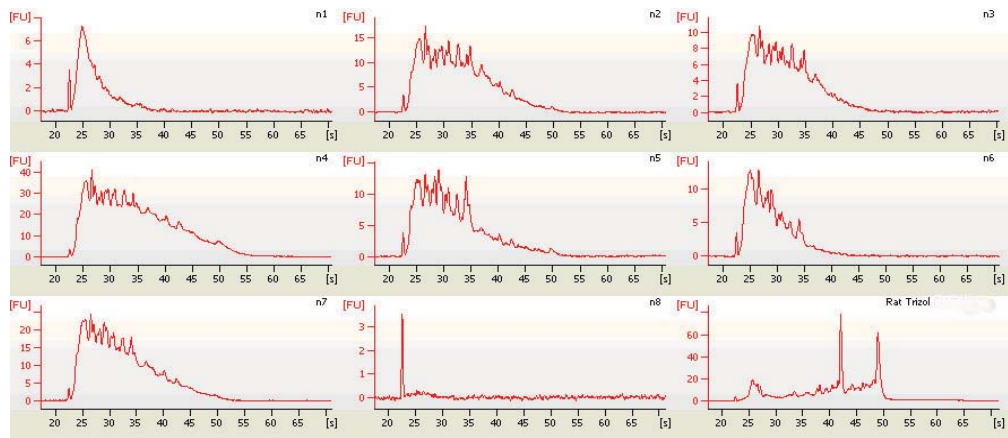


Figure 9.7: Electropherograms of RNA extracted from normal patient samples using Agilent Bioanalyzer 2100.

The analysis indicated substantial degradation of the samples.

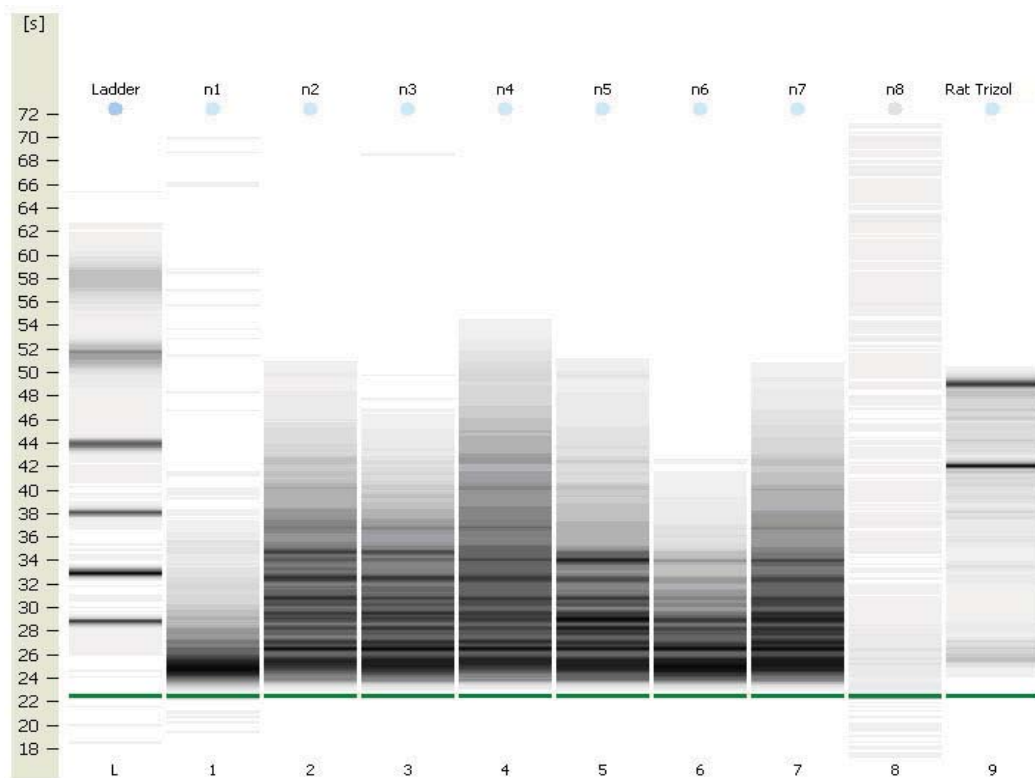


Figure 9.8: Gel images of RNA extracted from normal patient samples using Agilent Bioanalyzer 2100.

The analysis indicated substantial degradation of the samples.

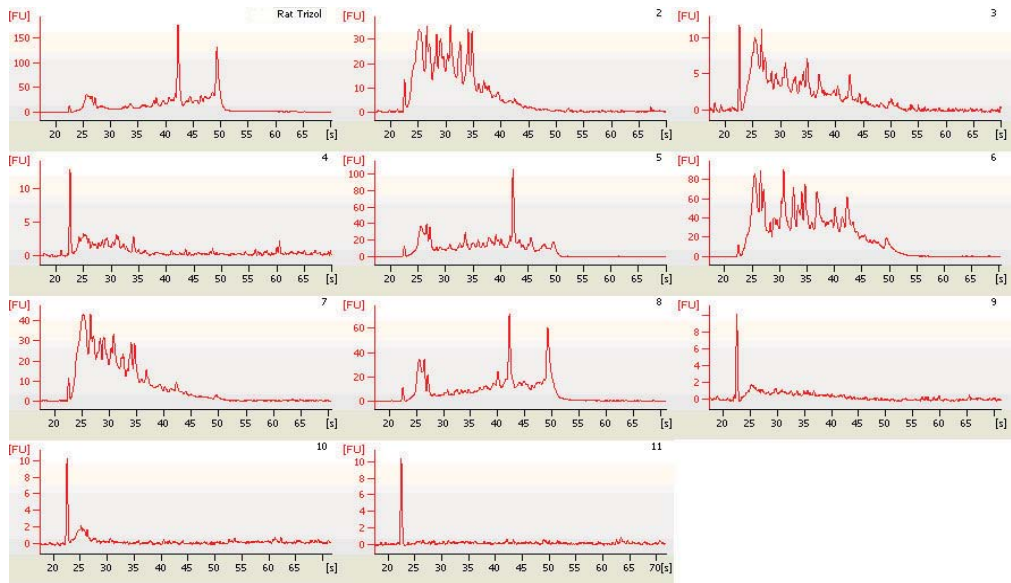


Figure 9.9: Electropherograms of RNA extracted from cancerous patient samples using Agilent Bioanalyzer 2100.

The analysis indicated significant degradation of the samples.

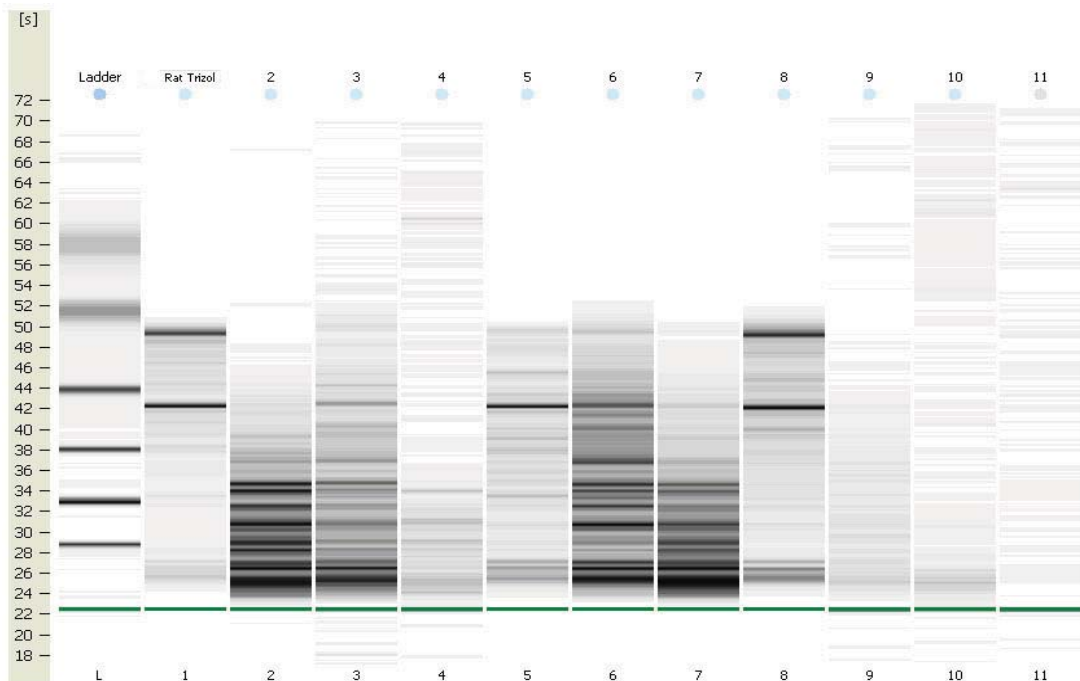


Figure 9.10: Gel images of RNA extracted from cancerous patient samples using Agilent Bioanalyzer 2100.

The analysis indicated significant degradation of the samples.